6. Environmental Context

HERVÉ MARTIN
Laboratoire Magmas et Volcans, Université Blaise Pascal, Clermont-Ferrand, France
(E-mail: martin@opgc.univ-bpclermont.fr)

PHILIPPE CLAEYS
DGLG-WE, Vrije Universiteit Brussel, Brussels, Belgium
(E-mail: phelaeys@vub.ac.be)

MURIEL GARGAUD
Observatoire Aquitain des Sciences de l'Univers, Université Bordeaux1, Bordeaux, France
(E-mail: gargaud@obs.u-bordeaux.fr)

DANIELE L. PINTI
GEOTOP-UQAM-McGill, Université du Québec à Montréal, Quebec, Canada
(E-mail: pinti.daniele@uqam.ca)

FRANCK SELSIS
Centre de Recherche Astronomique de Lyon and Ecole Normale Supérieure de Lyon, Lyon, France
(E-mail: franck.selsis@ens-lyon.fr)

Abstract. On Earth, the Archaean aeon lasted from 4.0 to 2.5 Ga; it corresponds to a relatively stable period. Compared with today, internal Earth heat production was several times greater resulting in high geothermal flux that induced the genesis of rocks such as komatiites and TTG suites, which are no more generated on Earth since 2.5 Ga. Similarly, the details of plate tectonic modalities (plate size, plate motion rate, plate thickness, tectonic style, irregular crustal growth, etc...) were different of modern plate tectonics. Both atmosphere and ocean compositions have been progressively modified and the greater heat production favoured the development of hydrothermalism and therefore created niches potentially favourable for the development of some forms of life. Catastrophic events such as giant meteorite falls or world-sized glaciations drastically and suddenly changed the environment of Earth surface, thus being able to strongly affect development of life. Even if specialists still debate about the age of the oldest indubitable fossil trace of life, Archaean can be considered as having been extremely favourable for life development and diversification.

Keywords: Archaean, continental growth, atmosphere and ocean evolution, meteoritic impacts, glaciations, young sun

After the Late Heavy Bombardment (see chapter 4.5), the Earth entered in a relative stability period that lasted until now. This does not mean that at 4.4 Ga, the Earth was similar to modern Earth, on the contrary, it was archaic and the internal as well as external processes were significantly different of those active on our modern Earth. For instance, if plate tectonics existed, the

detail of its modality (plate size, plate motion rate, plate thickness, irregular crustal growth, etc...) changed until today. Both atmosphere and ocean compositions have been progressively modified. All these changes, even if slow and progressive certainly had significant influence on the development and evolution of life on Earth surface. In addition to these progressive modifications, more punctual and/or catastrophic events took place, such as giant meteorite falls or world-sized glaciations. These events drastically and suddenly changed the environment of Earth surface, and even if they lasted a short period of time (at geological time scale), they also strongly affected development of life. The target of this chapter is to identify and describe these changes and to try to replace them in their temporal frame.

6.1. Evolution of Geological Mechanisms: The 2.5 Ga Transition

HERVÉ MARTIN

6.1.1. EPISODIC CRUSTAL GROWTH

Since more than 15 years, it has been clearly established that, if continental crust growth has been continuous, it was also a highly irregular process (Condie, 1989; McCulloch and Bennet, 1993; Condie, 1998). Figure 6.1 is based on two complementary approaches: estimate of crustal growth rates (McCulloch and Bennet, 1993) and compilation of crustal zircon ages (Condie, 1989; Condie, 1998). It shows that throughout the whole Earth history, crustal growth proceeded by super-events (i.e. 3.8, 2.7, 1.8, 1.1 and
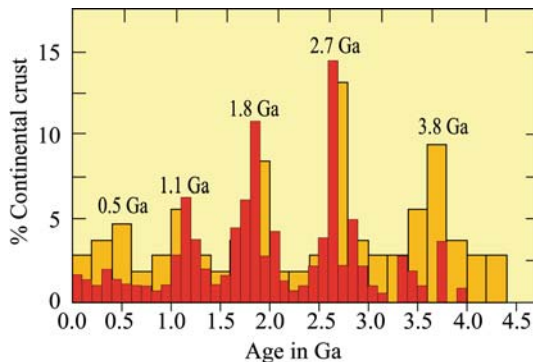

Figure 6.1. Histograms showing the estimated rates of crustal growth averaged over 200 Ma intervals (after McCulloch and Bennet, 1993, orange pattern) and the distribution frequency (100 Ma intervals) of U-Pb zircon ages (after Condie, 1989 and Condie, 1998, red pattern). This diagram clearly shows that the growth of continental crust has been a continuous but irregular process.

0.5 Ga). Typically each event lasted 250 to 350 Ma and is separated from the others by about 700−900 Ma.

Several authors consider that mantle plume activity could be responsible for the periodicity of Earth crust production (Stein and Hofmann, 1994; Albarède, 1998; Albarède, 2005). Albarède (1998) proposed that plume activity resulted in the emplacement of large oceanic plateaus, similar to the Mesozoic Ontong-Java plateau, where thick piles of plume basalts erupted on the oceanic floor. Indeed, when entering in subduction, these plateaus are able to undergo partial melting and to generate continental crust. For instance, today in Ecuador, the Carnegie ridge, which is generated by the Galapagos hot spot activity, is subducted under the South American plate since 5 Ma. There, the volcanic activity is more important than in other parts of Andes, the arc is larger and adakites are generated (Gutscher et al., 2000; Samaniego et al., 2002; Bourdon et al., 2003; Samaniego et al., 2005). This modern analogue testifies that increase of magmatic activity can result of basaltic plateau subduction.

Based on the Stein and Hofmann work (1994), Condie (1998) proposed an alternative model, which considers that in a subduction zone, the descending residual oceanic crust, transformed into eclogite, accumulates at the 660-km seismic discontinuity. When the amount of accumulated oceanic crust exceeds a threshold, it breaks the discontinuity and suddenly sinks into the mantle as a cold avalanche. These cold eclogites reach the mantle-core boundary (D'' layer) and take the place of the autochthonous warm mantle peridotite resulting in the uprising of a hot mantle plume. This catastrophic event can be considered as being a mantle and thermal overturn. As proposed by Albarède (1998) these uprising hot plumes can generate oceanic plateaus. Condie (1998) proposed that ascent of hot mantle mostly contributes to heat the upper mantle, which increases the rate of oceanic crust genesis, resulting in smaller and faster plates that enter more rapidly in subduction. Faster subduction of younger oceanic crust also results in increasing the rate of production continental crust (Martin and Moyen, 2002; Martin et al., 2005).

The downward motion of cold avalanches drags the overlying mantle, thus causing the development of "super subduction zones" above, which attract plates from great distances (Peltier et al., 1997; Condie, 1998). The convergence of the plates results in the growth of super continent. In fact, the development of super continents in these periods is due to two concomitant mechanisms: the collage and/or collision of pre-existing continental plates and the genesis of new juvenile continental crust due to subduction-related magmatic activity. Some of these supercontinents received names: Rodinia (1.1 Ga); Gondwana (0.5 Ga). Vaalbara has also been proposed for late Archaean (see: Condie, 1998; Zegers et al., 1998; Bourrouilh, 2001, for more details).

Moyen (1997) also evidenced the cyclic continent growth and evolution, which he divided into 4 stages. The first stage consists in arc complexes,

where continental crust is generated by melting of subducted slab (TTG and adakites) or of overlying mantle wedge (classic calc-alkaline magmas). During a second episode, arcs accrete due to collision or collage; this can be correlated to the cold avalanche as described by Condie (1998). The third stage consists in the reworking of the newly accreted crust. Indeed, genesis of juvenile continental crust also results in transferring and concentrating strongly incompatible elements such as U, Th and K from the mantle into the crust. These elements have radiogenic isotopes (^{235}U, ^{238}U, ^{232}Th, ^{40}K), whose decay contributes to heat the crust and thus, can help in its melting and recycling. The last episode is a quiescence period (may be partly due to the temporal impoverishment of the upper mantle in radioactive elements); which can evolve towards a new cycle or towards cratonization and development of thick and cold lithospheric keel.

   Existence of supercontinents has major influence not only in magmatic or deep geology, but also on climate and life. For instance, on a supercontinent fauna and flora will tend to homogenize and to follow a parallel evolution. After breakdown of such a continent, living being will evolve independently on their continental fragment.

6.1.2. Global evolution and changes (~2.5 Ga ago)

Taking into account the episodic and cyclic crustal growth could lead to the conclusion that the parameters of this cyclicity remained constant since the early Archaean. However, a rapid overlook of crustal composition through time points to major disparity between Early Archaean and Phanerozoic times. One of the more obvious differences consists in the temporal change in the nature and abundance of rocks. Some rocks are widespread in Archaean terrains whereas they are rare or inexistent after 2.5 Ga. This is the case for komatiites, TTG (Tonalite, Trondhjemite and Granodiorite) associations and Banded Iron Formations (BIF). Others, such as andesites, per-alkaline magmatic rocks and eclogites are abundant after 2.5 Ga and rare or unknown in Archaean terrains. In addition, others as high-Mg granodiorites (sanukitoids) are mainly known at the Archaean-Proterozoic boundary. Consequently, in superposition with cyclic crustal growth it exists an other secular evolution.

6.1.2.1. *Change in magma petrogenesis*
Typically, the main secular change in our planet history since its accretion is its progressive cooling. The more obvious evidence of this cooling is provided by komatiites (Figure 6.2). Komatiites are ultramafic lavas, which only exist in Archaean terrains. They were produced by high degrees of mantle melting ($\geqslant 50\%$) and they emplaced at temperatures ranging from 1525 to 1650 °C (Nisbet et al., 1993; Svetov et al., 2001) (today basalts are produced by 25 to 35% mantle melting at temperatures of about 1250−1350 °C). They
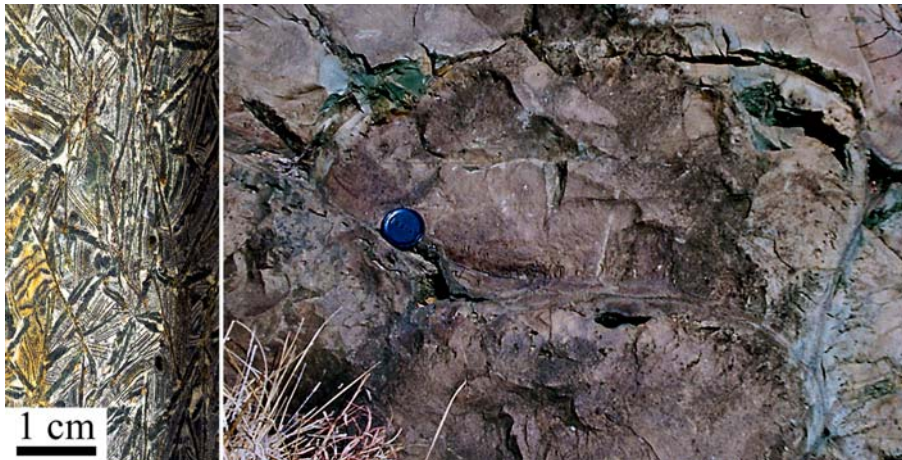
Figure 6.2. Right: 3.445 Ga old komatiitic pillow lava from the Hooggenoeg formation in Barberton greenstone belt (South Africa); Left: Typical spinifex texture in a 3.2 Ga old komatiite flow from Umburanas greenstone belt (Bahia state, Brazil). (Photos H. Martin).

corroborate that during the first half of Earth history, upper mantle temperature was greater than today. Since its formation, Earth cools such that after 2.5 Ga, it was not anymore able to reach high temperatures and consequently it became unable to produce high degrees of mantle melting, thus accounting for the disappearance of komatiites after Archaean times.

When Earth accreted, it accumulated energy, such as residual accretion heat, heat release by exothermic core-mantle differentiation, radioactive element (^{235}U, ^{238}U, ^{232}Th, ^{40}K) disintegration heat, etc. Since 4.55 Ga, this potential energetic stock is gradually consumed and consequently Earth progressively cools (Figure 6.3, Brown, 1985).

Archaean TTGs lead to the same conclusion. Indeed TTGs are generated by hydrous basalt melting, very probably in a subduction−like environment, where, due to high geothermal gradients, the subducted oceanic crust melts instead of dehydrating as it is today (Martin, 1986; Martin and Moyen, 2002). After Archaean times, dehydration of slab resulted in calc-alkaline andesites whereas, in mantle plume environments, per-alkaline magmas were generated by low degrees of mantle melting. Different estimates consider that Early Archaean mantle temperature was 100 to 200 °C greater than today.

6.1.2.2. *Sanukitoids*

At the Archaean Proterozoic (~2.5 Ga) boundary, huge volumes of high-Mg magmas emplaced that were called sanukitoids by Shirey and Hanson (1984). They possess petrologic and chemical characteristics intermediate between Archaean TTGs and modern calc-alkaline andesites (Figure 6.4). Recent works demonstrated that sanukitoids formed by partial melting of a mantle
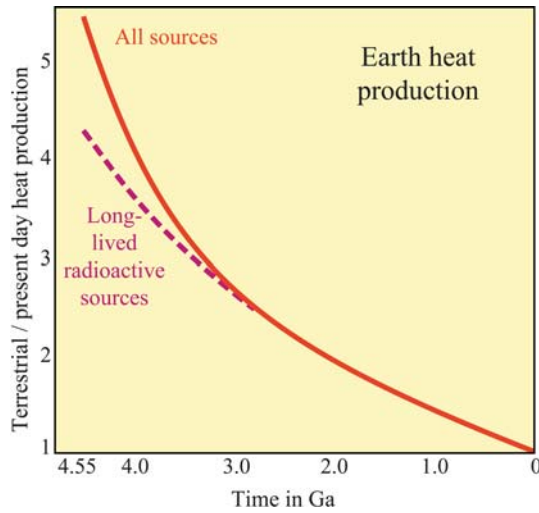
Figure 6.3. Temporal change of Earth heat production (after Brown, 1985).

Figure 6.4. 2.7 Ga old sanukitoids from Eastern Finland. Left: dyke of sanukitoid intrusive into the basic volcanics of the Kuhmo−Suomussalmi greenstone belt. Right: detail picture of sanukitoid, attesting of the abundance of feldspar megacrysts (white) in a matrix mainly made up of dark minerals (biotite and hornblende). (Photos H. Martin).

peridotite which composition has been modified by addition (metasomatism) of TTG magma (Smithies, 2000; Moyen et al., 2003; Rapp et al., 2003; Martin et al., 2005). In a subduction zone, the slab melts (TTG magma) have a low density and ascent through the overlying mantle wedge where they react with mantle peridotite. Rapp et al. (1999) established the concept of "effective melt/rock ratio": when this ratio is high, not all slab-melt is consumed during peridotite metasomatism and so, part of slab melt (TTG) reaches the continental crust. When the melt/rock ratio is low, all the slab
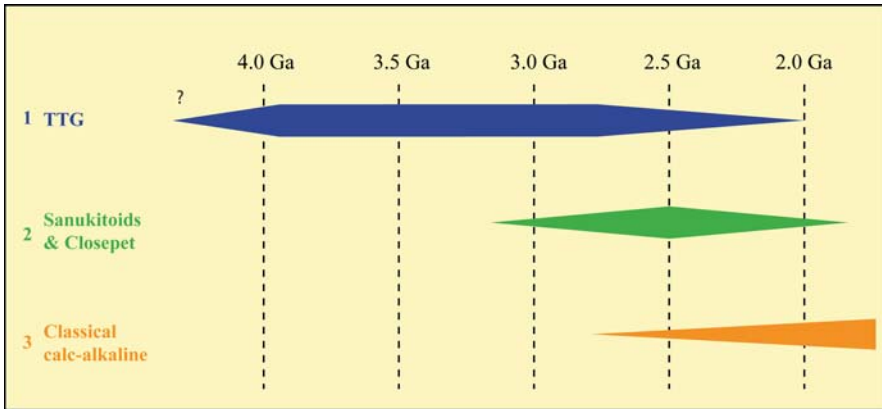
Figure 6.5. Schematic diagram illustrating the evolution of juvenile crustal magmatism in course of Earth history. The thickness of the colured domain is indicative of the volumetric importance of the magmatism. It clearly points to large domain of overlapping at the Archaean-Proterozoic transition (2.5 Ga).

melt is consumed in metasomatic reaction with the peridotite. Martin et al. (2005) proposed that sanukitoids represent transitional magmatism reflecting a major change in Earth thermal regime at about 2.5 Ga (Figure 6.5):

(1)   During Archaean times, Earth heat production was high leading to high degree of subducted slab melting. Consequently, during their ascent through the mantle wedge the melt/rock ratio was high such that part of slab melts reached the crust where they crystallized as TTG.

(2)   At the end of Archaean, Earth was significantly colder and consequently the degree of melting of subducted slab was low, resulting in a low melt/rock ratio. Therefore, the whole slab melts were consumed in reaction with mantle wedge, whose subsequent melting generated sanukitoids.

(3)   After 2.5 Ga, Earth was too cold to allow slab melting, so the subducted basalts cannot melt but only dehydrate and induce the melting of the overlying mantle peridotites, giving rise to the classical cal-alkaline magmas (andesites and granodiorites).

In other words, the sanukitoids are good markers of a major petrogenetic and thermal change in our planet. The fact that they mostly emplaced between 2.7 and 2.5 Ga allows to roughly dates this event.

6.1.2.3. *Change in tectonic style*
Changes did not occurred only in magma petrogenetic processes but also in global tectonic style. During Archaean times, modern-like horizontal
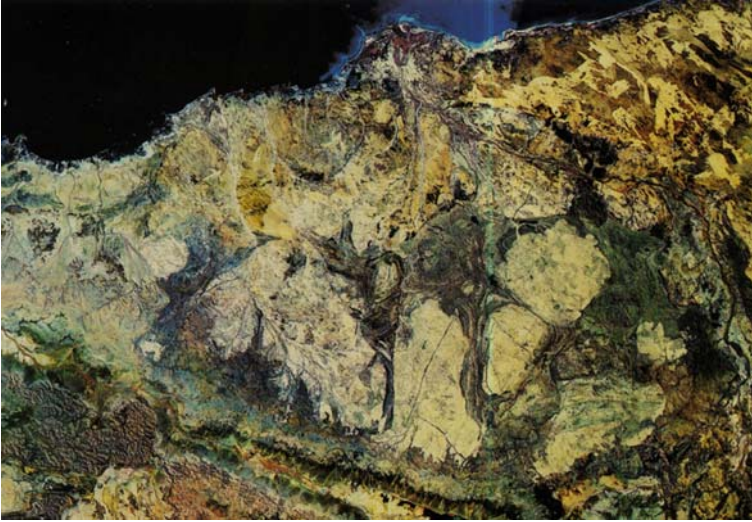
Figure 6.6. Satellite view of the 3.5–3.2 Ga old Archaean Pilbara block in Australia, showing the sagduction structures: the greenstone belts (dark green colour) are located in between TTG domes (white-yellow colours). The picture width is of about 450 km. (Photo Landsat).

tectonics operated and the large-scale horizontal structures (over-thrusts) resulted of continental collision events. However, vertical tectonics also appears in Archaean terrains whereas it is almost inexistent after 2.5 Ga. This tectonic style has been called sagduction by Gorman et al. (1978); it is a gravity driven tectonic, analogous to inverse diapirism (Figure 6.6). Indeed, when high density ($d = 3.3$) ultramafic rocks such as komatiites or even some iron-bearing sediments as BIF are emplaced over a low density ($d = 2.7$) continental crust made up of TTG, they generate a strong inverse density gradient leading to the down motion of high density greenstones into the TTG basement but also to the concomitant ascent of the surrounding low density TTG.

On Earth, the only high-density rocks able to emplace at the surface are komatiites and BIF. Today, most basalts have density that does not exceed 2.9 or 3.0. The resulting inverse density gradient is too low to initiate sagduction. As komatiites and BIF are restricted to Archaean times, vertical tectonics (sagduction) is also restricted to the primitive Earth crustal evolution.

6.1.2.4. *Juvenile vs. recycling*
Melting of the mantle or of a subducted oceanic crust generates felsic magmas that are extracted from the mantle; they contribute to increase the volume of the continental crust. This process is called a *juvenile* process. On the contrary, re-melting of older continental crust, generates new crustal magmas, but does not increase the continental crust volume. This mechanism is called *recycling*.

However, before to be able to recycle continental crust, it is necessary to create it. This is why, during Archaean times, juvenile processes were prominent and recycling was a subordinated process. Contrarily, after 2.5 Ga, the volume of continental crust was so great that recycling became prominent.

6.1.3. CONCLUSION

It appears that a very important period in Earth history has been the Archaean - Proterozoic boundary at about 2.7−2.5 Ga. It marks the change from archaic mechanisms before 2.5 Ga towards modern-like ones after. A single and simple cause can account for all the observed changes: the progressive cooling of our planet. However, the recorded change is relatively sudden and brutal whereas Earth cooling is a progressive mechanism. Consequently, we must invoke some threshold effect. This effect is well known in the case of felsic magmas (TTGs vs. calc-alkaline andesite). Indeed, a hydrous subducted oceanic slab melts at temperatures of about 700 °C; if it is dehydrated, it would only be able to melt for temperature greater than 1200 °C. Consequently, the threshold will be the geothermal gradient that will allow dehydration to occur for temperatures lower than 700 °C. Before 2.5 Ga, high geothermal gradients did not allow dehydration to occur prior to 700 °C, whereas today, lower geothermal gradients result in intense slab dehydration at temperatures lower than 700 °C.

The quick character of the change could have also been accentuated and reinforced by the genesis of a supercontinent at about 2.7 Ga. Figure 6.1 shows that this event was probably the more important ever recorder on our planet. Such a peak in crustal growth is accompanied by a huge transfer of heat producing radioactive elements from the mantle to the crust. One of the consequences is the warming of the crust leading to its intense recycling. However, another consequence is the important impoverishment of the upper mantle in these elements, which made it colder and significantly contributed in decreasing geothermal gradients, which could have accelerated the rapid character of the change.

Of course, these changes did not take place everywhere on Earth exactly at the same time. Indeed, for instance, today in subduction zones the geothermal gradient depends not only of the mantle temperature but also of the age of the subducted crust, the age of subduction, etc... (Martin, 1999). The value of these two last parameters can be highly variable, such that, for example, the age of oceanic crust when it enters in subduction ranges between 0 and 180 Ma. Consequently, locally calc-alkaline andesites were generated before 2.5 Ga whereas some TTG are known in Proterozoic terrains. However, it remains that most of the changes occurred after the 2.7 Ga supercontinent genesis, at about 2.5 ± 0.2 Ga.

6.2. Atmosphere and Ocean Physico-chemical Evolution

The presence of an atmosphere-hydrosphere early in the history of the Earth has been essential to life, mainly supporting synthesis of organic molecules, providing suitable ecologic niches (Nisbet and Sleep, 2001; Nisbet and Fowler, 2003), and regulating the climate (Sleep and Zahnle, 2001a; Zahnle and Sleep, 2002). Here, we report most recent hypothesis and the few direct and indirect evidences for the evolution of the atmosphere and hydrosphere during the Hadean and the Archaean eons. With the increasing geological record available after the 2.5 Ga transition, a description of the chemical evolution of the ocean and the atmosphere during Proterozoic and Phanerozoic times is a daunting work, well beyond the scope of this paper. A brief and updated account of the entire geological history of seawater and of the atmosphere can be found in (Holland, 2003).

6.2.1. Atmosphere evolution

Franck Selsis

6.2.1.1. *The prebiotic atmosphere*
By prebiotic, we refer to the era when life emerged on Earth. In order not to eliminate the possibility of interplanetary or interstellar panspermia, we consider here that life started to evolve on Earth during the prebiotic era, whether the origin of life origin was endogenous or extraterrestrial. A ''reference'' composition of the prebiotic atmosphere is given by Kasting (1993). This model describes the atmosphere around 3.8 Ga, a period closely bounded by the Late Heavy Bombardment (3.9−3.8 Ga) and the oldest plausible isotopic signatures of life (3.8 Ga) (Rosing, 1999). It is based on the following assumption:
- The composition of volcanic gases is roughly the same as it is today. This is supported by the composition of the oldest (~3.9 Ga) magmatic rocks (ultramafic lavas?) (Delano, 2001; Li and Lee, 2004).
- Molecular nitrogen has reached its present atmospheric level (PAL). This is consistent with the outgassing timing inferred from isotopes, with a ~30% uncertainty on the level of N_2 due to recycling between the atmosphere, the crust and the mantle (see part 4.3.1.4.).
- Carbonate-silicate regulation of the mean surface temperature (T_S) is at work (Walker et al., 1981). This requires the weathering of emerged continents and imposes a CO_2 level of about 0.2 bars. This point was debated by Sleep and Zahnle (2001b) who suggested that such high level of atmospheric CO_2 would be unstable due to the carbonitization of

basalts, which would maintain the early Earth in a globally frozen state. Efficient carbonitization of seafloor seems however inefficient when occurring below a km-thick frozen ocean. As carbonate-silicate recycling was shown to be the mechanism allowing the Earth to recover from Snowball events (Hoffman et al., 1998), it is reasonable to assume that it was also a mechanism able to overcome carbonitization and to sustain T_S above 0 °C.

The abundance of molecular hydrogen is obtained by balancing volcanic outgassing and Jeans escape of atomic H to space. Assuming a diffusion-limited loss to space, as in Kasting's original work, yields a H_2 mixing ratio of 10^{-3}. However, escape of atomic hydrogen in the modern oxic atmosphere is only limited by its diffusion above the tropopause because the exosphere is sufficiently hot (~1000 K). The high temperature of Earth's exosphere is due to its high O_2 and low CO_2 contents (the exosphere of Venus, for instance, remains below 278 K). The prebiotic atmosphere was anoxic and the low exospheric temperature, rather than diffusion, limited the loss of hydrogen. Tian et al. (2005) estimated the hydrogen loss and showed that a volcanic rate equal to the present one would result in an H_2 mixing ratio 100 times higher (0.1 bar). For higher volcanic rates (which are likely), molecular hydrogen can become the dominant species in Earth prebiotic atmosphere.

In the prebiotic atmosphere, O_2 is produced only by photochemistry and escape of hydrogen following H_2O photolysis, and maintained to a very low level ($<10^{-10}$) by reaction with reducing volcanic gases.

The abundance of methane depends on the efficiency of its abiotic production, which is assumed to originate from reducing hydrothermal fluids produced after serpentinization of ultramafic rocks. Today's abiotic production (mainly at off-axis mid-ocean ridges) released in an anoxic atmosphere would lead to mixing ratio below 10^{-6}. As a more extensive hydrothermal activity was likely at 3.8 Ga and because meteoritic impacts also contributed to the methane production (Kress and McKay, 2004), significantly higher levels of CH_4 (10^{-5}–10^{-4}) could be sustained (Kasting, 2005).

The composition in other gases is much more speculative: CO is often pointed as a major prebiotic gas because of its formation during impact and its abundance in the protosolar nebula. However, no quantitative study on the sources and sinks of CO are available. Nitrogen-bearing prebiotic compounds like HCN and NO can be produced by lightning and impacts at a rate critically depending on the level of the other gases, among which H_2, CO_2 and CH_4 (Navarro-Gonzalez et al., 2001; Commeyras et al., 2004).

This model likely represents average conditions on Earth at about 3.8 Ga if life was absent or only marginally involved in the global geochemical cycles. However, recent revisions of the impact history question this dating of

the prebiotic era at about 3.8 Ga. Earth became habitable after the last impact able to vaporize the whole ocean hit the Earth.[1] By triggering a magma ocean phase, such impact would not only annihilate the biosphere but also reset to simple molecules the complex organics that could have been formed before. By considering a monotonic decrease of the bombardment between the moon-forming impact and the dated lunar impacts, several authors estimated the rate of such catastrophes and the horizon for ancient life on Earth (Maher and Stevenson, 1988; Oberbeck and Fogelman, 1989; Sleep et al., 2001). They concluded that long lasting habitability started on Earth around 4.0 ± 0.1 Ga. As described in part 4.5, such monotonic decrease is not consistent with solar system formation models and the bombardment rate could have been comparable to the present one between the end of Earth accretion (~4.4 Ga) and the LHB (3.9 Ga; part 4.5). During the LHB itself, the Earth was bombarded by an integrated mass of asteroids lower than 1.8×10^{23}g (Gomes et al., 2005), which does not imply the occurrence of 500 km impactors (3×10^{12} Megatons) required to evaporate the entire oceans or 200 km bodies (10^{11} Megatons) able to warm it up to 100 °C. Therefore, and in the absence of constraints on the bombardment before 3.9 Ga, life could have emerged significantly earlier than previous hypotheses, as early as about 4.4 Ga. One of the main implications is that the prebiotic atmosphere may have been much more reducing that usually assumed. The composition of the atmosphere later than 4 Ga was the result of more than 500 Ma of irreversible oxidation through the escape of hydrogen to space, under the strong XUV irradiation of the early Sun (Selsis, 2004; Ribas et al., 2005), although hydrogen could still be abundant (Tian et al., 2005). H_2 and other reducing species including CH_4 could have dominated the very early atmosphere ~ 4.4 Ga ago (Sleep et al., 2004). It is important to insist that the uncertainty on the dating of the prebiotic atmosphere as well as on the dating of the oldest traces of life (see part 7.1) allows us to consider an origin of terrestrial life under a wide range of atmospheric composition: from H_2-, CH_4-rich to H_2, CH_4-poor.

6.2.1.2. The rise of O_2

Between 2.4 and 2.0 Ga, a change from global anoxic to oxic atmospheric conditions, the so-called "Great Oxidation Event" or G.O.E. (Holland, 2002), is revealed by several geological evidences (BIFs, red beds, palaeosols, detrital uraninite deposits) (Holland, 1994; Figure 6.7). It can now be dated with high precision thanks to sulphur isotopic enrichments recorded in rocks: Sulphur isotopes follow a "normal" mass-dependent fractionation for high

---

[1] This assumption is no longer true if life can survive such impact inside ejecta escaping the Earth and reseeding it after its recovery (Wells et al., 2003; Gladman et al., 2005).

levels of O_2 and "mass-independent" fractionation when this level is low. Mass-independent fractionation arises from the photolysis of SO_2 (Farquhar et al., 2000) in the absence of UV screening by O_3 and occurs at levels of O_2 below 10^{-5} PAL (Present Atmospheric Level) according to photochemical and radiative transfer modelling (Pavlov and Kasting, 2002). Mass-independent fractionation is found in all sediments between 3.8 and 2.32 Ga (Mojzsis et al., 2003). The partial pressure of O_2 increased from undetectable levels to more than 10^{-5} PAL at 2.32 Ga (Bekker et al., 2004). Palaeosols more recent than 2.2 Ga underwent oxidation at a level implying a minimum partial pressure of O_2 of 1-10 mbar, or 0.5−5% PAL (Rye and Holland, 1998). Although the quantitative inference of the partial pressure of O_2 from the composition of these palaeosols remains uncertain, palaeosols from 2.2−2.0 Ga seem to indicate a higher O_2 level (>5% PAL) than palaeosols from 1.8 to 0.8 Ga. One should keep in mind that these geological indicators may reveal local more than global conditions and can thus been affected by, for instance, locally enhanced biological release of O_2. Moreover, the average atmospheric level of O_2 is likely to have fluctuated due to complex biological, photochemical and climatic relationship between O_2, CO_2 and CH_4. Maybe more significant is the worldwide excursion of the $\delta^{13}C$ recorded between 2.25 and 2.05 Ga, which corresponds to the release of 10−20 times the present amount of atmospheric O_2 (Karhu and Holland, 1996). The existence of BIFs (Banded-Iron Formations; requiring reducing conditions) as late as 1.8 Ga, indicate that the deepest part of the ocean became oxic only 500 Ma

Figure 6.7. Banded Iron Formations (BIFs) from Sandur in India (Left) and from Kuhmo in Finland (Right); both are ~2.7 Ga old. The detail view on the right shows the alternations of quartz (white) and magnetite layers (black dark blue). (Photos H. Martin).

after the atmosphere (Holland, 1999). In fact, Anbar and Knoll (2002) showed that anoxic but sulphidic conditions in the deep ocean might still have prevailed after 1.8 Ga and as late as 0.6 Ga. Sulphur and carbon isotopes seem to indicate a second rise of O_2, from ~0.5% PAL to more than $5-20\%$ PAL around 0.7 ± 0.1 Ga ago (Canfield and Teske, 1996; Catling and Claire, 2005). The present level of O_2 was at least reached before the explosion of complex life took place (543 Ma) and probably around 0.6 Ga. The partial pressure of O_2 remained above 50% PAL during the entire Phanerozoic with a notable excursion to $150-200\%$ PAL ($350-400$ mbar) around 300 Ma (Permo-Carboniferous), associated with the rise of vascular land plants and the associated increase of carbon burial (Berner et al., 2003).

The question whether the appearance of oxygen producers coincided with the beginning of the great oxidation event or occurred much earlier is still open-ended. Molecular fossils of biogenic origins (hopanes and steranes) are a plausible indication for the existence of cyanobacteria and eukaryotes (the producer and consumer of O_2) at 2.7 Ga (Brocks et al., 2003b). Stromatolites built by phototrophs became abundant at about 2.8 Ga and exhibit similarities with modern stromatolites associated with cyanobacterial mats. Some of these stromatolites could result of non-oxygenic bacterial activity but Buick (1992) showed that at least some of them were not found in conditions allowing non-oxygenic photosynthesis. Isotopes of iron (Rouxel et al., 2005) and nitrogen (Shen et al., 2006) also exhibit changes at $2.7-2.8$ Ga, possibly indicating that oxygenation of the Earth was taking place at that time. Local oxidizing conditions found in 3.7 Ga sediments (Rosing and Frei, 2004) can be the result of an early biological oxygen release. If O_2 producers did appear as early as before 2.7 or even before 3.7 Ga, what is the cause of the delayed rise of atmospheric oxygen? Several mechanisms have been proposed:

(1)   The net release of atmospheric O_2 by photosynthesis is limited by the burial of organic carbon. Organic carbon that remains at the surface can eventually be oxidized, whether consumed by eukaryotes or directly exposed to atmospheric oxidants. It is thus possible that the rate of carbon burial, and thus the net release of O_2, has been kept at low values by early tectonics and then enhanced as result of the break-up of the Late Archaean Supercontinent after 2.3 Ga (Des Marais et al., 1992).

(2)   The build-up of O_2 can also be frustrated by the release of reducing volcanic gases when it exceeds the biological production of O_2. Kasting et al. (1993) proposed that, due to a progressive oxidation of the mantle, the balance might have favoured the accumulation of O_2 only after 2.3 Ga. However, the mantle redox required to produce such reducing volcanic gases is not consistent with the timing for the

degassing of nitrogen (Libourel et al., 2003; Marty and Dauphas, 2003) and no redox evolution is observed in lavas formed between 3.6 Ga and today (Delano, 2001; Li and Lee, 2004).

(3)   Unstable climate due to coexistence of widespread methanogens and emerging O_2 producers could have prevented the build-up of O_2 until solar luminosity increased to a high-enough value (Selsis, 2002).

(4)   Catling et al. (2001) suggested that methane-producing bacteria must have preceded the rise of O_2 by several hundred million years in order to enhance the escape of hydrogen to space and, consequently, the required irreversible oxidation of the Earth. However, considering the large hydrogen losses that occurred in the earliest history of the Earth (when the H_2-rich atmosphere was submitted to the strong solar XUV radiation, see Figure 6.8), it is unlikely that the hydrogen loss that occurred in the latest period predating the rise of O_2 contributed significantly to the total loss integrated since the formation of the Earth.
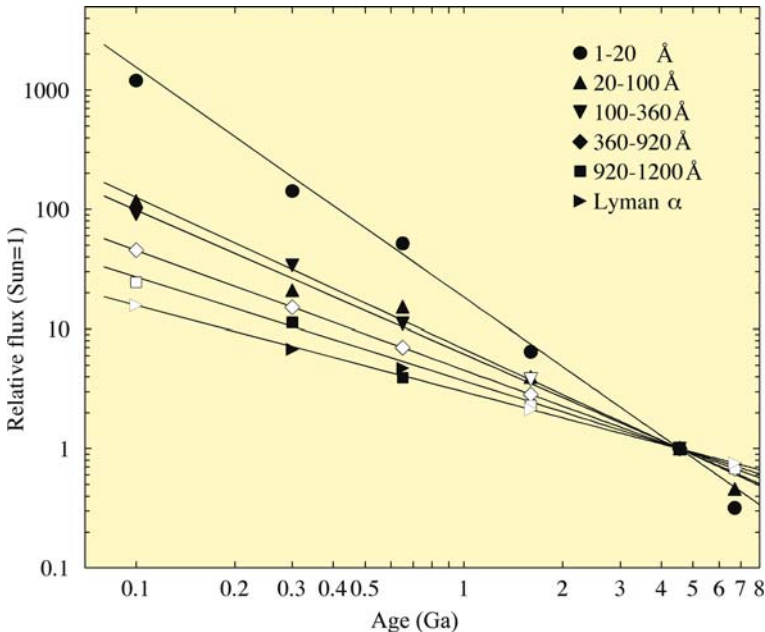
Figure 6.8. XUV emission from Sun-like stars at different ages. This graph represents the Solar-normalized fluxes measured in different wavelength intervals (filled symbols) from 6 Solar-type stars, EK Dra (0.10 Ga), $\pi1$ UMa and $\chi1$ Ori (0.30 Ga), $\kappa1$ Cet (0.65 Ga), β Com (1.6 Ga), β Hyi (6.7 Ga), and the Sun (4.56 Ga). The corresponding power-law fits are indicated. Empty symbols give the inferred flux where no observation is available. Adapted from Ribas et al. (2005).

According to Kopp et al. (2005), existing geological data and molecular fossils are still consistent with a late emergence of oxygen producers, around 2.3 Ga, that immediately triggered the great oxidation event, while for Melezhik et al. (2005) and Shen et al. (2006), oxygen-rich habitats associated with cyanobacteria undoubtedly existed before 2.7 Ga. The fascinating debate about the origins of oxygenic photosynthesis and its consequences on the whole planetary environment and on the biological evolution, remains extremely active. On this topic, we recommend two inspiring essays (Knoll, 2003; Catling and Claire, 2005).

6.2.1.3. *Evolution of the Sun and climate*

Standard models for the evolution of the Sun give a 37% increase of the luminosity between 4 Ga and present (Figure 6.9). If during this whole period, the Earth had the same atmosphere as today, (an obviously weak assumption) its surface would have remained globally frozen until about 2 Ga. Inversely, geological records prior to 2 Ga indicate that the Earth was warm before 2 Ga, with nearly no traces of glacial deposits except for the
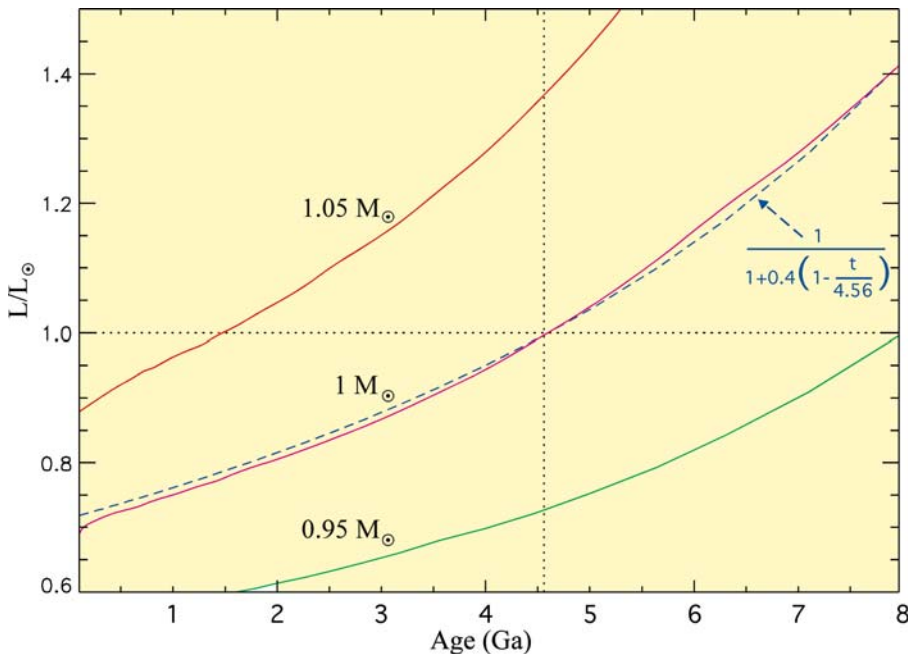

Figure 6.9. Evolution of the solar luminosity. This graph represents the evolution of the bolometric luminosity for 3 different stellar masses and solar metallicity (BCAH98-model-3 from Baraffe et al. 1998). The dashed curve shows a useful approximation for the solar evolution (Gough, 1981).

Pongola (2.9 Ga) (Nhleko, 2004) and Huronian polar glaciations (3 events between 2.45 Ga and 2.32 Ga) (Hilburn et al., 2005) and the Makganyene low-latitude glaciation (Snowball, 2.2 Ga) (Kopp et al., 2005, see part 6.3.2). This apparent contradiction, called the *faint young Sun problem* (Sagan and Mullen, 1972), is no longer a paradox once known that the atmospheric level of greenhouse gases (mainly CO_2) changed during Earth history (see Selsis, 2004, for alternative explanations of the faint young Sun problem). In particular, the atmospheric level of CO_2 is likely to be stabilized over geological periods by the carbonate precipitation (associated with the weathering of silicates) on one hand and the volcanic emission on the other (Walker et al., 1981). This climate regulation, which is assumed to work for Earth-like planets inside the circumstellar habitable zone (Kasting, 1993), can account for most of Earth's climate history. However, it could have been rendered inoperative in two ways. First, under very early tectonics, carbonate-silicate regulation may fail: efficient carbonitization of seafloor (Sleep and Zahnle, 2001b) could lead to surface temperatures below 0 °C while the lack of emerged continents to provide silicate weathering could lead to a build-up of CO_2 and surface temperatures well above 0 °C. Second, the release and consumption of atmospheric gases by the biological activity can overrule the carbonate-silicate regulation. In particular, methanogenesis, known as a very primitive metabolism, could have sustained a warm climate before the rise of oxygen (Pavlov et al., 2000; Kasting, 2005). In the absence of atmospheric O_2, the present production rate of CH_4 by methanogens would result in 100 to 1000 times the present atmospheric abundance of methane (1 PAL = 1.6×10^{-6}). To illustrate the efficiency of CH_4 as a greenhouse gas, let us consider that the atmosphere of the Earth at 2.8 Ga had the same composition as today, except for O_2, assumed to be absent (for practical reasons, we assume a 1 bar partial pressure of N_2 to compensate for the lacking 0.2 bars of O_2). The present level of CO_2 (3×10^{-4}) would be too low to sustain a temperature above 0 °C: even with 1 PAL of CH_4, the average surface temperature would be around −10 °C. If we keep the CO_2 level to 1 PAL and we increase the CH_4 to 10, 100 and 1000 PAL, the surface temperature would rise to 0 °C, 5 °C and 15−20 °C, respectively (Pavlov et al., 2000). Moreover, under anoxic conditions, methanogens can colonize most of the habitable environment, while on modern Earth they can grow only under anaerobic conditions, like the ones found in swamps, in hydrothermal systems and in the digestive system of mammals. Even higher levels of atmospheric methane, and higher surface temperatures, are thus likely to have occurred between the emergence of methanogens (at an unknown date) and the great oxidation event (2.3 Ga), although there is no geological evidence to support this hypothesis. At very high levels of CH_4, 1) photochemical hazes start to form like in Titan atmosphere, resulting in an enhanced albedo and 2) CH_4 begins to absorb a significant part of the visible

and near infrared solar radiation, producing a stratospheric warming that reduces the surface warming (again like on Titan). For a given level of CO_2, there is thus a limit of the surface temperature that can be reached under a CH_4-rich atmosphere. This limit is however not well determined due to incomplete spectroscopic data of CH_4 and uncertain properties of these hazes, but it could certainly be as high as 30 °C for 1 PAL of CO_2 at 2.8 Ga.

If the emergence of O_2 producers occurred when CH_4 was the main greenhouse gas, climatic consequences would be dramatic: the photochemical lifetime of atmospheric CH_4 drops, anoxic conditions required by methanogens became scarcer yielding a decrease of the production rate of CH_4, and CO_2 consumption increases due to the enhanced biological productivity. Therefore, the beginning of O_2 production is likely to trigger a glaciation or even a snowball[2] event. Under snowball conditions, oxygenic photosynthesis "freezes" while CH_4 and CO_2 can rise again. Under low solar irradiation, such configuration (competing CH_4- and O_2-producers) can induce a steady state characterized by a temperature slightly above 0 °C and a very low abundance of O_2 ($<10^{-5}$). Such steady state is however unstable and can result in repeated glaciations (Selsis, 2000). The collapse of a CH_4-warming is the favoured explanation for the earliest identified snowball (Makganyene glaciation, 2.3−2.2 Ga) (Kopp et al., 2005). The three Huronian glaciations (probably restricted to low-latitudes, Hilburn et al., 2005), which shortly predated the Makganyene event, and the Pongola Glaciation (2.9 Ga) could be caused by such instabilities if oxygen producers were already widespread.

After the great oxidation event, atmospheric levels of methane were limited by the growing oxic environment and by the short photochemical lifetime of CH_4 but could have remained a major greenhouse gas, with a level exceeding 10 PAL (Pavlov et al., 2003). Therefore, the Neoproterozoic Snowball, associated with a second rise of O_2 could have also been triggered by the fall of the CH_4 abundance down to about its present level.

---

[2] Snowball glaciations, characterized by an ice cover down to the equator, are the coldest times recorded in Earth's history. At the beginning of these events, the runaway ice-albedo feedback makes the global mean temperature drop to −50 °C for a few tens of thousands of years (Schrag et al. 2002). This temperature drop is followed by a period of a few million years during which the mean temperature is around −10 °C. Earth recovers from Snowball events thanks to the carbonate-silicate regulation (Hoffman et al., 1998): volcanic gases released in the absence of surface liquid water and carbonate precipitation, allow CO_2 to build-up to a level high enough to warm the surface above 0 °C.

6.2.2. CHEMICAL EVOLUTION OF THE OCEANS

DANIELE L. PINTI

6.2.2.1. *Hadean (4.6−3.8 Ga)*

The chemistry of seawater in the early Hadean was likely controlled by high-temperature water−rock interactions between the hot $CO_2−H_2O$ runaway greenhouse and the basaltic proto-crust (see part 4.2.2.2). Modern analogues of these environments could be mid-oceanic ridges. At mid-oceanic ridges, due to water circulation, rocks partially dissolve thus saturating water in the major constituents of the rock. Similarly, in the early Earth, magma eruption repeatedly brought basalts into contact with the atmospheric water vapour, maintaining its saturation in major elements (Sleep et al., 2001). Today, similar atmosphere-rock reactions are supposed to take place at the surface of Venus (Johnson and Fegley, 2002). When the runaway greenhouse cooled down, possibly before $t_0 + 165$ Ma (see part 4.2.2), condensed seawater started to penetrate deeper in the oceanic basaltic proto-crust, experiencing extensive water−rock interactions. A significant difference with modern seawater is that CO_2 was an abundant volatile in the early runaway atmosphere making early oceans more acidic than today (pH = 5.5, Pinti, 2005). Attack of such solutions on exposed rock was thus more rapid, enriching the solution of dissolved salts (Krauskopf and Bird, 1995).

The first volatile to condense was chlorine, likely outgassed from the Earth's interior in the form of HCl (Holland, 1984; Graedel and Keene, 1996). The amount of chlorine available at the beginning is difficult to evaluate. Holland, (1984) considered that H_2O and Cl were both degassed from the interior of the Earth. Using the Cl/H_2O ratio in the crust, Holland, (1984) calculated an amount of 24.8 g/Kg_{water}, which represents 1.2 times the present value (18.8 g/Kg_{water}). This figure is probably a minimum estimate, and it is expected that higher concentrations of chlorine were available in the primordial oceans. Amounts of chlorine 2 times the present values have been argued by Knauth (1998, 2005), based on mass balance calculations including chlorine from evaporite deposits of marine origin, recycled and deposited on the continental crust during Proterozoic and Phanerozoic times.

The amount of available Na in early seawater was by far enough to combine with Cl to form NaCl. Sodium was removed from the basaltic proto-crust, through pervasively hydrothermal-driven water−rock interactions. As an example, a global layer of basalt of 500-meter thick could supply the total amount of Na actually present in the modern ocean (Sleep and McClure, 2001; Sleep et al., 2001). Continuous genesis and recycling of cooled lava at the surface of the planet could have thus supplied the amount of sodium required for saturating the primordial ocean with a NaCl-dominated brine. Depending on the pressure, solid NaCl may have been

in equilibrium with a water–rich high-pressure gas (representing the proto-atmosphere, Pinti, 2005). Temperature and pressure conditions necessary for the transition from two fluids to one fluid plus solid NaCl were 407 °C, at 298 bars (Bischoff and Rosenbauer, 1988).

Other abundant cations were likely K^+, Ca^{2+} and Mg^{2+}. Particularly, Ca^{2+} and Mg^{2+} should have been more concentrated than today due to the higher pH of the primitive oceans, since at low pH they exist together with HCO_3^-. The Ca^{2+}/Mg^{2+} ratio could have been higher than today because it was likely controlled by the reactions with basalts at mid-ocean ridges (Bischoff and Dickson, 1975). Sulphate ion would have been scarce or absent, because sulphur was mainly under its reduced form (Krauskopf and Bird, 1995). Rarer metals whose concentrations at present are kept low by reactions with and such as Ba^{2+}, Sr^{2+} and Mn^{2+} likely played a more important role in Hadean seas (Krauskopf and Bird, 1995; Holland, 2002; Holland, 2003). Halogens could have been also abundant, mainly bromine and iodine, because the absence of a biosphere able to scavenge them from seawater and fix on sediments, as occurs today (Krauskopf and Bird, 1995; Channer et al., 1997). The lower rates of sedimentation expected for a Hadean planet dominated by oceans, with small continental plates and very small or no emerged continent, should have favoured the concentration of halogens in seawater. Finally, in a poorly oxygenated and acidic early ocean, iron was very abundant as soluble ferrous iron (Fe^{2+}) (Holland, 2003, and references therein).

During Hadean, high salinities, together with high temperatures (Knauth and Lowe, 2003), could have limited the hypothetical biological activity in the sea (Knauth, 2005). Complex organic molecules are indeed vulnerable to damage caused by sodium and chlorine in seawater and only organisms adapted to these "drastic" conditions, such as extremophiles, could have developed and survived (Cowen, 2005; Knauth, 2005).

6.2.2.2. *Archaean (3.8–2.5 Ga)*

Major advances in the comprehension of the chemical evolution of the oceans come from two main sources: indirect evidence derived from the mineralogy of sediments of that period (see: Holland, 1984; Holland, 2003, for a detailed analysis) and from the isotopic fractionation of elements sensitive to the redox of their depositional environment (mainly sulphur and nitrogen, Beaumont and Robert, 1999; Farquhar et al., 2000; Farquhar et al., 2001; Pinti et al., 2001; Shen and Buick, 2004). Direct evidence for the chemical composition of seawater is rather scarce in the Archaean sequences and mostly derived from a very few chemical analyses carried out in fluids inclusions into minerals which are considered to have preserved pristine seawater (Channer et al., 1997; de Ronde et al., 1997; Appel et al., 2001; Foriel et al., 2004; Weiershauser and Spooner, 2005).

Indirect evidence of the chemical properties of seawater and of its redox state comes mostly from the study of the few carbonates and Banded Iron Formation (Figure 6.7) (Holland, 1984; Isley, 1995; Holland, 2002; Konkauser et al., 2002). The carbonate minerals in Archaean sediments are mainly calcite, dolomite, aragonite and scarce siderite ($FeCO_3$). This latter mainly occurs in the Banded Iron Formations (Holland, 1984). This means that the oceans were supersaturated in Ca^{2+} and Mg^{2+}, but estimation of their concentrations is difficult to achieve (Holland, 2003). A rough upper limit of 250 for the Ca^{2+}/Fe^{2+} ratio in the Archaean seawater has been derived by Holland (2003) from the absence of significant siderite fraction in the BIF. This value is much lower than the present-day Ca^{2+}/Fe^{2+} ratio in seawater of 9.1×10^6 (Horibe et al., 1974; Gordon et al., 1982). In the modern oxygenated ocean, Fe^{3+} is rapidly precipitated as $Fe(OH)_3$. The higher Fe^{2+} concentrations observed in the Archaean indicates a much lower O_2 content in the atmosphere and in the near-surface ocean. The higher Fe^{2+} and Mn^{2+} contents found in Archaean limestones, compared to their Phanerozoic counterparts (Veizer et al., 1989), support this hypothesis.

Stronger evidences of a poorly oxygenated ocean come from the isotopic fractionation of elements such as sulphur and nitrogen. In the absence of O_2, solar UV interact with SO_2 and generate large mass-independent fractionation (mif) of sulphur isotopes ($\delta^{33}S$) in the reactions products (sulphides and sulphates, Farquhar et al., 2000). The mass-dependent fractionation of the sulphur isotopes ($\delta^{34}S$) in sedimentary sulphides is smaller prior to 2.7 Ga (less than 20%) than in more recent times, when variations of 20% to 40 % are measured. This has been interpreted as the result of a lower concentration of sulphate in the Archaean seawater (0.2 mMol L^{-1}) compared to the present-day (28.7 mMol L^{-1}), which inhibited isotopic fractionation during sulphate reduction (Holland, 2002). In the absence of oxygen, pyrite would not have been oxidized during weathering, reducing drastically the concentrations of sulphates in the Archaean ocean. Nitrogen isotope ratios ($\delta^{15}N$) measured in Archaean (older than 2.7 Ga) organic matter (Beaumont and Robert, 1999; Pinti et al., 2001; Pinti et al., 2003; Ueno et al., 2004), show two distinct populations centred around $\delta^{15}N$ values of −3.6 and +4.3, respectively (Shen et al., 2006). Negative nitrogen isotopic values have been interpreted by Beaumont and Robert (1999) as the result of an Archaean nitrogen oceanic cycle different from the modern one, and dominated by nitrogen fixation in a poor-O_2 environment. Alternatively, Pinti et al. (2001) interpreted these values as representative of a marine N cycle dominated by biological cycling of reduced N species by chemolithotrophs at hydrothermal vents, suggesting a chemistry of the ocean largely buffered by interactions with the mantle (see: Shen et al., 2006, for a detailed synthesis).

Direct evidence for the chemical composition of seawater is rather scarce in Archaean sequences. Some studies suggest that pristine fluid inclusions,

containing Archaean seawater, could have been preserved in the geological record (Channer et al., 1997; de Ronde et al., 1997; Appel et al., 2001; Foriel et al., 2004; Weiershauser and Spooner, 2005) (Table 6.1). Appel et al. (2001) studied quartz globules preserved in pillow basalts from localized low-strain domains of 3.75 Ga sequences at Isua Greenstone Belt, West Greenland. Fluid-gaseous inclusions in quartz globules contain remnants of two independent fluid/mineral systems including pure CH_4 and highly saline aqueous fluids (about 25 wt.% NaCl equivalent), and co-precipitating carbonates (calcite). Appel et al. (2001) interpreted this aqueous system as a relic of sea-floor hydrothermal fluids (Table 6.1). However, the salinity of modern venting solutions is close of that in modern seawater (3.5 wt% equivalent NaCl), deviating by 40−200% from the average only at specific vents (0.4−7 wt% equivalent NaCl, von Damm et al., 1995). The high salinities measured in these inclusions (10 times the modern hydrothermal systems) may have been produced by Archaean seawater, with salinity 3 times the present value, modified by high temperature hydrothermal reactions with basalts (Appel et al., 2001). Alternatively, phase separation could have been produced during prograde metamorphism of the rocks, leaving an enriched saline residual in the inclusions. Isua sequences are indeed highly metamorphosed, at amphibolite facies ($T460 − 480$ C and 4 kb), and it cannot be excluded that phase separation could have affected the fluid content of these inclusions.

High salinities have also been observed in primary fluid inclusions from intra-pillow quartz from the North Pole Dresser Formation (3.490 Ga), Pilbara craton, Western Australia (Foriel et al., 2004). These rocks never experienced high-T metamorphism ($T \leq 200$ °C). The chemistry of the fluid inclusions, particularly the Cl/Br ratios, point to the occurrence of at least three fluids: a saline fluid (Cl/Br = 631 and a 12 wt% equivalent NaCl); a Fe-rich fluid (Cl/Br = 350); and a Ba-rich fluid (Cl/Br = 350). The saline fluid is likely seawater (Foriel et al., 2004). The Cl/Br ratio of 630 is indeed very close to that of modern seawater (Cl//Br = 647). The amount of chlorine, 4 times the present value, is explained by intense evaporation of seawater. The Fe-rich and Ba-rich fluids have Cl/Br ratios close to bulk Earth value (420), possibly indicating mantle buffering (Channer et al., 1997; de Ronde et al., 1997) and a hydrothermal origin for these fluids. This seems to be corroborated by the occurrence of nitrogen and argon having a pure pristine mantle signature in intra-pillow cherts from the same formation (Pinti et al., 2003; Shen et al., 2006). The Dresser formation sequence at North Pole has been interpreted as an estuarine littoral sedimentary deposit with a stratified body of deeper water enriched of primary hydrothermal barium and silica emanating from white smokers (Nijman et al., 1998; Van Kranendonk et al., 2001). Therefore, it appears logic to find a mixing between evaporated seawater and hydrothermal fluids, in these inclusions.

TABLE 6.1

Chemistry of Archaean, Paleoproterozoic seawater and hydrothermal fluids, together with that of Na–Ca–Cl brines from Precambrian Shields

Location	Age Ma	Stratigraphy	Type of inclusion/ sample name	Cl⁻ mmol/L	Br⁻ mmol/L	SO₄²⁻ mmol/L	Na⁺ mmol/L	K⁺ mmol/L	Mg²⁺ mmol/L	Ca²⁺ mmol/L	Sr²⁺ mmol/L	Cl/Br mmol/L	Type of fluids
North Pole, W. Australia	3490	Warrawoona; Dresser Fmt	Metal-depleted[1] (Pi0l-21)	2284	3.8	n.d.	n.d.	49.1	n.d.	525	3.7	596	Seawater
North Pole, W. Australia	3490	Warrawoona; Dresser Fmt	Metal-depleted[1] (Pi02-39/1)	1772	2.7	n.d.	n.d.	44.4	nd	385	2.4	642	Seawater
North Pole, W. Australia	3490	Warrawoona; Dresser Fmt	Metal-depleted[1] (Pi02-39/2)	2580	4.2	n.d.	n.d.	78.0	n.d.	679	4.3	607	Seawater
North Pole, W. Australia	3490	Warrawoona; Dresser Fmt	Metal-depleted[1] (Pi02-39/3)	2065	3.4	n.d.	n.d.	52.1	n.d.	486	3.0	652	Seawater
North Pole, W. Australia	3490	Warrawoona; Dresser Fmt	Iron-rich[1]	2580	4.2	n.d.	n.d.	78.0	n.d.	679	4.3	402	Hydrothermal
North Pole, W. Australia	3490	Warrawoona; Dresser Fmt	Barium-rich[1]	1599	4.0	n.d.	n.d.	603.9	n.d.	437	3.5	370	Hydrothermal
Ironstone Pods, RAS	3230	Fig Tree Group	Seawater end-member[2]	920	2.3.	2.3	789	18.9	50.9	232	4.5	409	Seawater
Ironstone Pods, RAS	3230	Fig Tree Group	Hydrothermal end-member[2]	730	2.6		822	21.5		43	0.2	282	Hydrothermal
Ironstone Pods, RAS	3230	Fig Tree Group	Seawater end-member[2]	758	2.4	n.d.	n.d.	n.d.	n.d.	n.d.	n.d.	313	Seawater
Griqualand West, RAS	2220	Transvaal; Ongeluk Fmt	Quartz (Bosch Aar)	33538	262.0	185	6446	605.0	164	12258	316.0	128	Hydrothermal
Griqualand West, RAS	2220	Transvaal; Ongeluk Fmt	Quartz (Bosch Aar)	11559	95.0	46	2178	201.0	45	4160	99.0	122	Hydrothermal
Griqualand West, RAS	2220	Transvaal; Ongeluk Fmt	Qtz-II (Bovenongeluk)	1675	16.4	42	283	60.0	n.d.	n.d.	n.d.	102	Seawater

TABLE 6.1
Continued

Location	Age Ma	Stratigraphy	Type of inclusion/ sample name	Cl^- mmol/L	Br^- mmol/L	SO_4^{2-} mmol/L	Na^+ mmol/L	K^+ mmol/L	Mg^{2+} mmol/L	Ca^{2+} mmol/L	Sr^{2+} mmol/L	Cl/Br mmol/L	Type of fluids
Griqualand West, RAS	2220	Transvaal; Ongeluk Fmt (Bovenongeluk)	Qtz-II	4190	38.9	87	869	160.0	n.d.	n.d.	n.d.	108	Seawater
Griqualand West, RAS	2220	Transvaal; Ongeluk Fmt (Bovenongeluk)	Qtz-I	8084	68.0	87	1333	88.0	n.d.	n.d.	n.d.	119	Seawater
Griqualand West, RAS	2220	Transvaal; Ongeluk Fmt (Bovenongeluk)	Qtz-I	14716	108.1	50	4532	476.0	n.d.	n.d.	n.d.	136	Seawater
Griqualand West, RAS	2220	Transvaal; Ongeluk Fmt (Bovenongeluk)	Qtz-I	753	6.1	47	211	10.0	n.d.	n.d.	n.d.	123	Seawater
Griqualand West, RAS	2220	Transvaal; Ongeluk Fmt (Bovenongeluk)	Qtz-I	5429	38.6	35	1098	120.0	n.d.	n.d.	n.d.	141	Seawater
Griqualand West, RAS	2220	Transvaal; Ongeluk Fmt (Bovenongeluk)	Qtz-I	1513	10.9	34	343	13.0	n.d.	n.d.	n.d.	139	Seawater
Precambrian Shields			Ca–Na–Cl Brines[4]	1520	6.2	2.89	468.78	2.5	28.19	498	4.7	244	Brine
Precambrian Shields			Na–Ca–Cl Brines[5]	383	1.0	1.01	277.14	2.6	4.61	65	0.5	379	Brine
Modern seawater			Na–Cl-dominated	556	0.9	28.7	477	10.1	54.2	11	0.1	647	Seawater

Note.

1. Average have been weighted by the number of inclusions analyzed. The average values are slightly different from those calculated by Foriel et al. (2004).

2. As calculated by de Ronde et al. (1997).

3. Average of 27 analyses from Charmer et al. (1997).

4. Average from 26 analyses of brines from Finland, Sweden and Canada, as reported by Frape it al. (2003).

5. Average from 16 analyses of brines from Finland, Sweden, Canada, UK and West Europe as reported by Frape et al. (2003).

However, the fact that seawater could have evolved in a closed basin does not help in determining its initial saline content.

De Ronde et al. (1997) studied the fluid chemistry of what they believed to be Archaean (3.2 Ga) seafloor hydrothermal vents. Quartz crystals found in iron oxide structures (Ironstone Pods) from the 3.5−3.2 Ga Barberton greenstone belt, South Africa, contain fluid inclusions, which may derive from a mixing between a $NaCl−CaCl_2$ dominated seawater and a $CaCl_2−FeCl_2$ hydrothermal fluid. The Na/Cl ratio in this presumed Archaean seawater is the same as the present-day ocean (0.858), but the total amount of sodium and chlorine is 1.6 times the present day value (Table 6.1). The concentrations of Ca^{2+}, Sr^{2+} are 22 and 50 times higher than the present-day ocean, possibly, because the more acidic ocean did not allow them to precipitate as carbonate, as today. The concentration of is lower than in modern seawater because sulphur was largely in reduced form (Krauskopf and Bird, 1995; Holland, 2003). Finally, the Cl/Br ratio of 400 is very close to the bulk Earth value (420) and of those observed at mid-oceanic ridges, suggesting that halogens were buffered by mantle. Lowe and Byerly (2003) have recently contested the Archaean age of these deposits, showing that the Ironstone Pods are largely composed of goethite (a thermally unstable hydrated iron oxide mineral), deriving from quaternary dissolution of the Archaean siderite. The debate that followed is casting doubts on the validity of these data, which were considered the most compelling evidence of the chemistry of the Archaean seawater.

Very recently, Weiershäuser and Spooner (2005) reported the chemistry of primary fluid inclusions in quartz-filled vesicles and interstitial and drainage cavity quartz from pillowed flows in the area of Ben Nevis, in the 2.7 Ga Abitibi Greenstone Belt, Ontario, Canada. They measured salinities in what they assumed to be Archaean seawater, ranging from 4.8 to 11.4 wt% equivalent NaCl with a small subset of inclusions yielding salinities between 20 and 25 wt% equivalent NaCl. These results point out again the possible higher salinity of the Archaean ocean compared to modern seawater. Three main hypothesis can account for high salinities in fluid inclusions: (1) Younger high saline fluids of unknown origin were trapped and erroneously interpreted as primary, modified high-salinity seawater; (2) phase separation occurred, leaving a highly saline brine as the liquid phase (which got trapped in the inclusions), and a low-salinity vapour phase, which escaped the system before trapping could occur; and (3) a pristine Archaean high-salinity seawater was trapped (Weiershauser and Spooner, 2005).

The first hypothesis seems not plausible. There are compelling mineralogical evidence that the structures, where the fluid inclusions reside, are primary structures. They are mostly undisturbed by post-deposition metamorphism (de Ronde et al., 1997; Foriel et al., 2004; Weiershauser and Spooner, 2005), with the possible exception of inclusions from Isua (Appel et al., 2001). Weiershäuser and Spooner (2005) argued against phase separation, because there is no

evidence of liquid and vapour-dominated inclusions in the same fluid inclusion assemblages, which will be the rule for samples affected by boiling (Roedder, 1984). Although assuming these fluid inclusions as pristine seawater, several questions can be raised. Do these inclusions give a real representation of the early global ocean? Alternatively, do the high salinities recorded in these inclusions reflect local conditions, such as close basins, where seawater was affected by high degree of evaporation? This latter hypothesis, for example, seems to be the likely explanation for the high salinities observed in the North Pole aqueous inclusions (Foriel et al., 2004).

Salinity of Archaean fluids could have been strongly modified by interactions with the volcanic pile at seafloor, prior to be definitively trapped in rocks. Several of these inclusions contain Na−Ca−Cl dominated fluids, which are characteristics of deep continental water circulating or having interacted with the crystalline basement (Frape et al., 2003). Ca−Na−Cl and Na−Ca−Cl brines, with salinities 10 times the modern seawater, have been found in most Precambrian shields, in Finland, Sweden, Russia and Canada (Fritz and Frape, 1987; Frape et al., 2003, and references therein). In (Figure 6.10), we reported the concentrations of dissolved species, normalized to those found in modern seawater, for Archaean seawater (de Ronde et al., 1997), Palaeoproterozoic seawater (Gutzmer et al., 2003) and the average composition of Ca−Na−Cl and Na−Ca−Cl-dominated brines (calculated from compiled literature data from Frape et al., 2003). Except for a lower K^+ and Mg^{2+} amount in Ca−Na−Cl brines, the variations in dissolved species and the dilution-enrichment factors of these brines are very close to those estimated for the Archaean seawater. Deep-brines from Precambrian shields have been interpreted, based on their H, O, Cl and Sr isotopic ratios, as derived from intense evaporation of modern-like seawater. Prolonged water−rock interactions are thus responsible for their variations in the dissolved species (Frape et al., 2003). The resemblance with Archaean seawater may suggest that early oceans had chemistry and Total Dissolved Salinity (TDS) practically identical to modern seawater. Most of the variations in the amounts of dissolved species (Figure 6.10) could be thus derived from seafloor water−rock interactions or contamination by hydrothermal fluids and may not reflect a different chemistry of the early oceans. Further studies on this issue are needed to answer to this hypothesis.

It is only in Proterozoic terrains that fluid inclusions with a chemistry similar to that of modern seawater is finally found. Palaeoproterozoic aqueous inclusions found in 2.22 Ga pods and short veins of quartz within basaltic andesites of the Ongeluk Formation, Transvaal Supergroup, South Africa, show the presence of Ca-rich high saline fluids, resulting from water−rock interactions with the host volcanic rocks together with seawater having a NaCl concentration equivalent to that of modern seawater (~4 wt% equivalent NaCl, Gutzmer et al., 2003). This could indicate that the
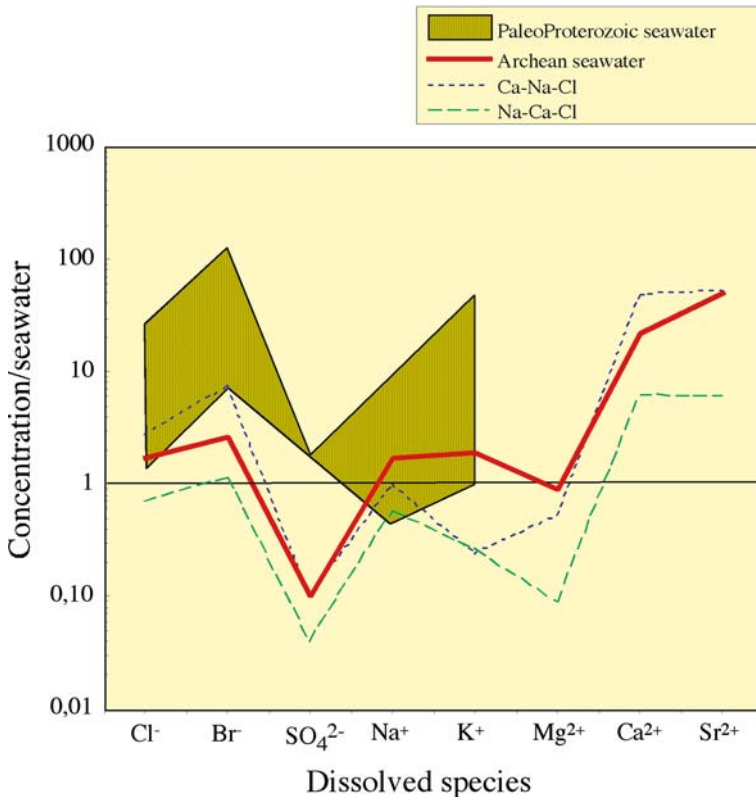
Figure 6.10. Concentration of dissolved anions and cations in Archaean and Paleoproterozoic seawater (data from de Ronde et al., 1997 and Gutzmer et al., 2001, respectively) normalized to the concentrations in modern seawater. Seawater-normalized average concentrations of Ca−Na−Cl and Na−Ca−Cl-dominated brines flowing in crystalline Precambrian shields of Finland, Sweden, Russia and Canada are also reported for comparison (data from Frape et al., 2003).

chemistry of seawater was starting to evolve towards the present-day conditions, just after the 2.5 Ga transition. However, Knauth (2005) suggested that the first great lowering of oceanic salinity probably occurred in latest Precambrian (ca. 1 Ga ago), when enormous amounts of salt and brine were sequestered in giant Neoproterozoic evaporite basins.

Gutzmer et al. (2003) measured Cl/Br values in 2.22 Ga inclusions and found that they are similar to those predicted for Archaean seawater (bulk Earth value), but significantly below to those of the present-day seawater. Gutzmer et al. (2003) suggested that ambient seawater in continental shelf environments at ca. 2.22 Ga was still buffered by vent fluids. This conclusion seems to be common in most of the Archaean studies: the chemistry of the Archaean ocean was buffered by the mantle, through emission of dissolved chemical species and volatiles from mid-oceanic vents and high-temperature pervasive water−rock interactions throughout the oceanic crust. Only with

the progressive build up of larger continents and of an abundant biosphere in Proterozoic times, riverine input and biological controls start to regulate the chemistry of seawater (Veizer and Compston, 1976; Veizer et al., 1989; Channer et al., 1997; Kamber and Webb, 2001; Pinti, 2005, and references therein).

This high saline ocean could have been warmer than today. Oxygen isotope data for early diagenetic cherts (Figure 6.11) indicate surface temperatures of about 55−85 °C throughout the Archaean (Knauth and Lowe, 1978; Knauth, 1998; Knauth and Lowe, 2003), but these data are actually controversial (see Pinti, 2005, and references therein). Data from fluid inclusions suggest a temperature of 39 °C at 3.2 Ga (de Ronde et al., 1997). Because O_2 solubility decreases strongly with increasing temperature and salinity (Weiss, 1970), the Archaean hotter and highly saline ocean has been probably maintained anoxic, even if atmospheric O_2 were somehow as high as 70% of the modern level (Knauth, 2005).

6.3.   Disturbing Events

PHILIPPE CLAEYS

Among the brutal events capable of modifying the environment of life on Earth surface are meteoritic impacts and glaciations. If most Archaean and

Figure 6.11. 3.445 Ga old chert from the Hooggenoeg formation in Barberton greenstone belt (South Africa). This chert is considered as formed due to hydrothermal activity in an environment possibly similar to modern mi-ocean ridges. Chemical analyse of such rocks provides information on water composition at the time of their formation. (Photo H. Martin).

Proterozoic impact craters disappeared due to erosion and plate tectonics, their traces are preserved in sedimentary records, as spherule layers. Similarly, glaciation periods strongly affected the environment and modified exogenous mechanisms such that their existence and influence have also been imprinted in the sedimentary record.

6.3.1. SPHERULE LAYERS: THE RECORD OF ARCHAEAN AND PROTEROZOIC IMPACT EVENTS.

Among the ~175 impact structures known on Earth, only a small fraction is Proterozoic in age, but this fraction includes two giants: Sudbury in Canada (~250 km in diameter and 1.850 Ga old) and Vredefort in South Africa (estimated to reach 300 km in diameter and dated at 2.023 Ga). So far, no crater of Archaean age has been identified, and due to the limited amount of preserved lithologies of this age, it is rather unlikely that one will ever be found. It is undeniable that also during this period, asteroids and/or comets were colliding with Earth. The ejecta layers recorded in ancient sedimentary sequences constitute the only remaining trace of these early impacts. These layers are generally composed of particles ejected during the cratering process, transported for hundreds to thousands of km and deposited in sedimentary sequences. When an extraterrestrial body collides with the Earth, a huge amount of energy is released leading to the vaporization and melting of both the projectile and the upper parts of the target-rock. The cratering process is accompanied by the ejection of target-rock debris as solid, vapour and molten phases. These different impact products are recorded in sedimentary sequences as distinct ejecta layers containing shocked minerals, spherules made of glass (or its alteration product) and crystallites, Ni-rich spinels, and/or geochemical anomalies (such as the famous positive anomaly in Iridium and in other Platinum group elements).

The study of Phanerozoic ejecta, especially at the Cretaceous-Tertiary (KT) boundary, demonstrates that rounded millimetre-sized spherules constitute the type of ejecta by far easiest to recognize in the field. The spherules originate by the melting or vaporization of the target-rock and of part of the projectile. They condense or quench in flight, inside or outside the upper atmosphere, before landing back at distal sites from the impact point. The spherules are usually rounded but other aerodynamically shaped morphologies such as elongated, teardrops or dumbbells are also frequent. Smit et al. (1992) and Smit (1999) have discussed in detail the characteristics and geographic distribution of the different types of spherules occurring in the KT boundary layer. Two kinds of spherules are classically distinguished: (a) spherules containing crystallites of clinopyroxene, spinels and olivine and called microkrystites (Glass and Burns, 1988); they most likely condensed out

of the vapour plume generated by the impact; (b) spherules entirely made of glass and called microtektites, which result from the melting of the upper part of the target-rock and subsequent rapid quenching in flight. Another didactic example exists in the Late Eocene with two closely spaced layers of microkrystites and microtektites respectively produced by the Popigai and Chesapeake Bay impacts (see Montanari and Koeberl, 2000, for review).

The current record of spherule layers of Archaean and Proterozoic ages is presented in Table 6.2. Ten ejecta layers crop out in Western Australia and South Africa; they concentrated in two time-windows between 2.65 to 2.50 Ga and 3.47 to 3.24 Ga. Few ejecta layers are known outside these two ''impact windows''. Between 2.13 and 1.84 Ga, Chadwick et al. (2001) identified a single unit rich in impact spherules, reaching maybe 1 m thick, in dolomitic sediments of the Ketilidian orogenesis in West Greenland (Figure 6.12). Recently, the probable ejecta layer produced by the Sudbury crater, was recognized in several sections of the uppermost part of the Gunflint Formation near the US–Canadian border in Minnesota and Ontario (Addison et al., 2005). Dated between 1.88 and 1.84 Ga, this ~50 cm thick ejecta unit contains shocked quartz and impact spherules. The younger (Late Proterozoic, 0.59 Ga) ejecta produced by the Acraman crater in Australia is described by Wallace et al. (1990). So far, only the ejecta layers found in some of the least metamorphosed and tectonised sedimentary units of the Barberton Greenstone Belt in South Africa (Lowe et al., 2003, for review) and of the Hamersley Basin in Western Australia (Simonson, 2003, for review) allow drawing some interesting hypotheses relevant for the ancient record of impact events.

Proterozoic and Archaean spherule layers are most likely to be preserved when deposited below the zone of surface wave influence, in rather deep-water environments of the continental shelf. In such low-energy environments, they avoid reworking and the absence of bioturbation ensures that they remain undisturbed. The known ejecta layers commonly occur in beds coarser than the surrounding units, interpreted as due to high energy depositional episodes, perhaps related to tsunamis or massive sediment transports triggered by the impact (Hassler et al., 2000; Hassler and Simonson, 2001; Simonson and Glass, 2004). Because they are free of burrowing and/or reworking by organisms, the Archaean and Proterozoic ejecta units provide a clear view of their depositional process and sorting. It is likely that both spherule-types are represented in some of these ancient layers.

Today K-feldspar, sericite, chlorite, quartz and carbonate have replaced the original spherule composition (Lowe et al., 2003; Simonson, 2003). The highly resistant dendritic spinels probably represent the only primary crystals preserved in the early to middle Archaean spherules of the Barberton Greenstone Belt (Byerly and Lowe, 1994). At the KT boundary, dendritic spinels formed either by condensation out of the impact induced vapour

TABLE 6.2
Main spherule layers recorded in Archaean and Proterozoic terrains, Modified after Simonson and Glass (2004)

| Layer	Location	Formation	Age (Ga)	Lateral extend (km)	Layer thickness (cm)	Accumulation spherules (cm)	Spherule size (mm)	Ir (ppb)
Acraman	South Australia, Adelaide Geosyncline, Officer Basin	Bunyeroo, Rodda beds	0.59	700	0–40	Traces	1.0	2.0
Sudbury	Ontario Minnesota	Gunflint-Rove boundary Biwabik-Virginia boundary	1.84–1.88	260	25–70	?	?	n.d
n.n	Southern Greenland	Vallen Group, Graenseso	2.13–1.85	26*	100	20	1.4	<DL
n.n	Western Australia Hamersley basin	Dales Gorge Member of Brockman	2.48	135	30	6.0	2.1	19.9
n.n	Western Australia Hamersley basin	Wittenoom	2.54	330	10–100	3.5	1.1	0.43
n.n	South Africa Griqualand West basin	Reivilo	2.56 ?	25	2–20	1.8	1.3	n.d
n.n	Western Australia Hamersley basin	Carawine**	2.63 ?	75	940–2470	30.0	2.3	1.54
n.n	Western Australia Hamersley basin	Jeerinah**	2.63	160	0.3–280	7.0	2.0	11.4
n.n	South Africa Griqualand West basin	Monteville**	2.60–2.63	230	55	5.0	1.6	6.4
S4	South Africa, Barberton belt	Mapepe	3.24	Single outcrop	15	7.5	1.6	450
S3	South Africa, Barberton belt	Mapepe and Unlundi	3.24	30	15–200	10.0	4.0	725
S2	South Africa, Barberton belt	Mapepe	3.26	12	20–310	10	2.5	3.9
S1	South Africa, Barberton belt	Hooggenoeg	3.47	25	10–35	5.0	1.0	3.0
	Pilbara craton Western Australia	Apex Basalt**		1	110	7.5	0.8	n.d
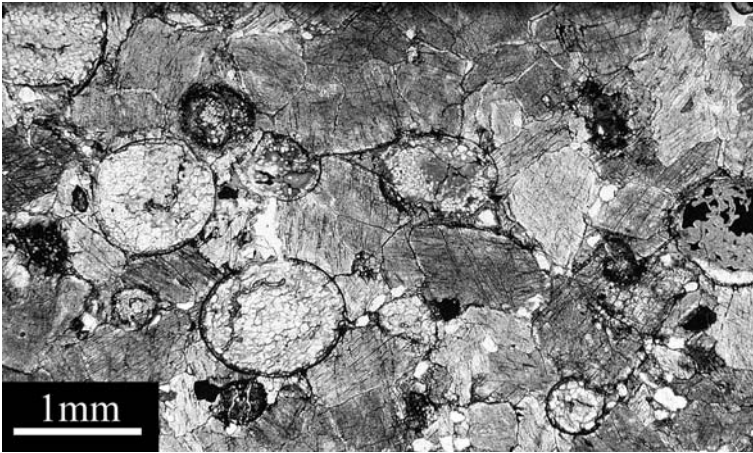
Figure 6.12. Polarized light microphotograph of spherules in a dolomitic matrix. These spherules come from the Ketilidian orogenesis (2.1–1.8 Ga) in Greenland. (Photo Ph. Claeys).

cloud (Kyte and Bostwick, 1995) or by the fusion and oxidation of the impacting projectile during its passage through the atmosphere (Robin et al., 1992). Although being of indisputable impact origin, the Barberton spinels differ in composition from their Phanerozoic counterparts; they are enriched in Cr, depleted in Mg and have higher Ni/Fe ratio. Their significantly lower Fe^{3+}/Fe_{total} ratio is consistent with their formation in the Archaean oxygen-poor atmosphere (Byerly and Lowe, 1994).

The ejecta layers exposed in the sedimentary sequences of the Barberton Group (South Africa), and of the Hamersley Basin (Western Australia) present some major differences with the ejecta units recognized in the Phanerozoic. These ancient layers contain thicker spherule accumulations and their composition seems to be more mafic than their Phanerozoic equivalent. Simonson and Harnik (2000) estimate that the spherule concentration is 10 to 100 times greater than that measured in the Phanerozoic ejecta. Most layers are a few centimetres thick but some can reach 30 cm (Table 6.2). In the most recent layers, pure spherule accumulations are barely thicker than 0.1 cm, except for the KT boundary and that only at proximal sites to the Chicxulub crater (Smit, 1999). The ejecta layer found in the 2.6 Ga Wittenoom formation of the Hamersley basin (Australia) maintains a consistent thickness of several cm over more than 20,000 km^2 (Simonson, 1992; Simonson and Harnik, 2000), while other layers probably extend over several hundreds of km (Simonson et al., 1999). In Western Australia, the Jeerinah ejecta layer of the Hamersley Basin is correlated with the Carawine horizon in the Oakover river region of the Pilbara Craton to the East and possibly with the layer occurring in the Monteville Formation of South Africa. If such correlations are reliable, they imply that the area of spherule

distribution was greater than 32,000 km^2 (Simonson et al., 1999; Rasmussen and Koeberl, 2004; Simonson and Glass, 2004). The possibility of a global distribution of these ejecta debris certainly deserves to be considered. Based on the Phanerozoic record, a crater of ~100 km in diameter is probably capable of spreading ejecta worldwide. The location of their source craters is of course unknown, but based on the spherule accumulation and consistency over important distance, Simonson et al. (199) interpreted them as rather distal (deposited > 5 crater radii) ejecta layers.

The size of these ancient spherules ranges between 1 and 4 millimetres. Meteoritic contamination of these layers is generally quite significant (Lowe et al., 2003). The reported Iridium concentrations range from a few ppb (equivalent to most KT boundary sites) up to values of 725 ppb for one of the Barberton layers (Table 6.2). Chromium isotopes (^{53}Cr/^{52}Cr) indicate that the projectile responsible for the formation of the Carawine and Jeerinah spherules likely corresponded to an ordinary chondrite, while the S4, S3, and S2 layers were probably formed by the fall of carbonaceous chondrites (Shukolyukov et al., 2000; Shukolyukov et al., 2002; Kyte et al., 2003).

Based on texture and overall composition, the Archaean and Proterozoic spherules were probably originally basaltic. Due to secondary replacement, it is difficult to estimate their primary composition. However, it appears that in many spherules, the replacement occurred with (some) preservation of the original texture. The K-feldspar crystals commonly display a typical elongated and fibrous lath-shaped morphology that resembles that formed by the rapid cooling of basaltic glasses (Simonson and Harnik, 2000). In other spherules now containing calcite, quartz or chlorite pseudomorphs, quenched and devitrification textures can still be recognized along with botroydal shapes and flow-bands (Simonson, 2003). Phanerozoic spherules are most commonly replaced by smectite and their chemistry rather reflects the composition of the continental crust. So far, only one sample of the Jeerinah layer in Western Australia contains shocked quartz grains (Rasmussen and Koeberl, 2004). The mafic character of the Archaean and Proterozoic spherules, combined with the scarcity of shocked quartz has been interpreted as the result of impacts on the oceanic crust (Lowe et al., 2003; Simonson, 2003). Oceanic impacts are further substantiated by the occurrence of many spherules in high-energy sedimentary units that could be caused by a major disturbance of the water masses during deposition (Hassler and Simonson, 2001; Lowe et al., 2003; Simonson et al., 2004). The dominance of oceanic impacts agrees with the suggestion that before 2.5 Ga the volume of oceanic crust was more important than the present-day 60% (McCulloch and Bennett, 1994). In the Phanerozoic oceanic impacts are rare, mafic ejecta is exceptional, and so far no crater is known to have excavated the oceanic crust (Dypvik et al., 2003). The apparently common cratering of the oceanic crust

in the Archaean and Proterozoic may be explained either by very large projectiles or by much shallower oceans than in the Phanerozoic, or both.

It thus seems likely that collisions the size of the KT event, or even significantly bigger, took place during two distinct intervals between 3.47 to 3.24 Ga and 2.65 to 2.5 Ga. The thickness of the ejecta, − if indeed they are distal layers −, the rather large dimension of spherule, and mass balance estimations based on the concentration of Ir and extraterrestrial Cr, − assuming the global distribution of the ejecta −, all these evidences indicate that the projectiles responsible for the formation the S2, S3, S4 Barberton impact layers varied between 20 and 50 km in diameter (Lowe et al., 2003). These sizes imply the formation of craters between 400 and 1000 km in diameter, quite bigger than Chicxulub, Sudbury or Vredefort. Simonson et al. (1999) also advocates that large projectiles, KT equivalent or more, formed some of the younger impact layers identified in Western Australia.

The clustering of spherule layers between 3.47 to 3.24 Ga and 2.65 to 2.5 Ga might be due to the coincidental preservation of two exceptional periods marked by a higher delivery rate of large impactors. It could also be interpreted as evidence that the whole Archaean and Early Proterozoic period was marked by a high flux of projectiles on Earth. The latter is compatible with the dating of lunar spherules that documents a progressive decrease in the collision frequency, after the end of the Late Heavy Bombardment 3.8 Ga ago (Culler et al., 2000, see discussion in Claeys, chapter 4.5). Glikson (2001) speculated that the Barberton dense spherule record coincides with a possible spike of impacts on the Moon around 3.2 Ga. These impacts could have influenced the evolution of early life, affected the oceans/atmosphere system or even modified the plate tectonic regime. Large oceanic impact could evaporate part of the ocean, and/or the associated disturbance could contribute to the mixing of a strongly stratified ocean increasing the exchange of nutriment-rich waters (Lowe et al., 2003). Glikson (1999; 2001) has speculated that they also lead to crustal deformation, rifting, fracturing of the crust, massive volcanism and uplift. The on-going searches for ejecta deposits at other stratigraphic levels in the Archaean and the Proterozoic should provide answers to some of these questions.

6.3.2. THE PALEOPROTEROZOIC GLACIATIONS, THE FIRST SNOWBALL EARTH

The first evidence for possible mid-latitude glaciations occurs in the diamictite of the Pongola Supergroup in South Africa, which is dated at about 2.9 Ga (Young et al., 1998; Nhleko, 2004) unfortunately few studies have been devoted to them. Between 2.45 and 2.22 Ga, three episodes of glaciations are recorded in the Huronian Supergroup of Canada (Hilburn et al., 2005). From oldest to youngest, diamictite deposits are present in the Ramsey

Lake, the Bruce and the Gowganda Formations. The precise ages of these events remain poorly constrained. The Nipissing diabase, dated at 2.22 Ga, crosscuts the entire Huronian sequence. Therefore, the Gowganda diamictite must be older than 2.2 Ga, as it is covered by km-thick sediments belonging to the Lorrain, Gordon Lake and Bar River Formations (Kopp et al., 2005). Based on the existing paleomagnetic data, the latitudinal extension of the three Huronian glacial deposits cannot be defined (Kopp et al., 2005). At this point, it is thus difficult to compare them with the Late Proterozoic glaciations, which probably covered the whole planet leading to the concept of Snowball Earth (Hoffman et al., 1998). Moreover, the Huronian glacial sediments do not seem to be covered by warm water carbonates (the so-called cap carbonates) (Kopp et al., 2005), which in the Late Proterozoic are indicative of an abrupt transition to much warmer climates.

Recent isotopic dates and new correlations indicate that the glacial deposits occurring in the Transvaal Supergroup of South Africa probably postdate the Huronian diamictites (Kopp et al., 2005). The Bosheok diamictite cropping out in the eastern part of the Transvaal region probably correlates with the Makganyene diamictite deposited in the Griqualand region, to the west of the Transvaal Basin. A Re-Os age of 2.3 Ga has been established for the Timeball Hill formation that is found below the Boshoek diamictite (Hannah et al., 2004). The Makganyene glacial deposits are interfingered with the Ongeluk marine basalt. The latter correlates with its subaerial equivalent the Hekpoort volcanics, which contains zircons, dated at 2.2 Ga (Cornell et al., 1996). Paleomagnetic data acquired on the Ongeluk basalts imply that the Makganyene glacial unit was deposited at tropical latitude, around $11° ± 5°$ (Evans et al., 1997). Based on this stratigraphy and low latitude occurrence, Kopp et al., (2005) advocated that the Makganyene event represents the oldest evidence for global glaciation, in other words, the first case of a Snowball Earth in the history of the planet.

The origin of oxygen producing cyanobacteria remains a major topic of discussion (see part 7.1). Several organic Biomarkers, traces of microfossils – considered by some authors as controversial –, the presence of stromatolites and isotopic fractionation, which origin has been debated, have widely been used as indicators of oxygen production by organisms since 2.8 Ga or even as early as 3.7 Ga (see Brocks et al., 1999; Des Marais, 2000; Catling et al., 2001; Brasier et al., 2002; Brocks et al., 2003a; Rosing and Frei, 2004). However, the significant mass independent fractionation of sulphur isotopes detected only in Archaean and Palaeoproterozoic sulphides supports an atmospheric oxygenation taking place only 2.5–2.2 Ga ago (Farquhar et al., 2002; Farquhar and Wing, 2003). The presence of only a few percent of oxygen in the lower atmosphere would hamper the penetration of the light of wavelength under 200 nm responsible for the photolysis of SO_2 to S, which results in the fractionation of S isotopes (Farquhar et al., 2001).

The presence of thick red beds, lateritic paleosols and major Mn deposits indicative of oxygen conditions occurs immediately below or above the Makganyene glacial deposits. This succession let Knopp et al., (2005) to propose that O_2-producing cyanobacteria appeared just before the Makganyene glaciation, between 2.3 and 2.2 Ga. The active oxygenic photosynthesis would have induced the rapid collapse of the pre-existing methane greenhouse leading to a Snowball event on a time scale of ~1 Ma (Kopp et al., 2005).

References

Addison, W. D., Brumpton, G. R., Vallini, D. A., McNaughton, N. J., Davis, D. W., Kissin, S. A., Fralick, P. W. and Hammond, A. L.: 2005, *Geology* **33**(3), 193−196.

Albarède, F.: 1998, *Tectonophysics* **296**, 1−14.

Albarède, F.: 2005, in M. Gargaud, P. Claeys and H. Martin (eds.), *Des atomes aux planètes habitables*, Presses Universitaires de Bordeaux, Bordeaux, pp. 79−102.

Anbar, A. D. and Knoll, A. H.: 2002, *Science* **297**, 1137−1141.

Appel, P. W. U., Rollinson, H. R. and Touret, J. L. R.: 2001, *Precambrian Res.* **112**, 27−49.

Baraffe, I., Chabrier, G., Allard, F. and Hauschildt, P. H.: 1998, *Astron. Astrophys.* **337**, 403.

Beaumont, V. and Robert, F.: 1999, *Precambrian Res.* **96**(1−2), 63−82.

Bekker, A., Holland, H. D., Wang, P.-L., Rumble III, D., Stein, H. J., Hannah, J. L., Coetzee, L. L. and Beukes, N. J.: 2004, *Nature* **427**, 117−120.

Berner, R. A., Beerling, D. J., Dudley, R., Robinson, J. M. and Wildman, R. A. Jr: 2003, *Ann. Rev. Earth Planetary Sci.* **31**, 105−134.

Bischoff, J. L. and Dickson, F. W.: 1975, *Earth Planetary Sci. Lett.* **25**, 385−397.

Bischoff, J. L. and Rosenbauer, R. J.: 1988, *Geochim. Cosmochim. Acta* **52**, 2121−212.

Bourdon, E., Eissen, J.-P., Gutscher, M.-A., Monzier, M., Hall, M. L. and Cotten, J.: 2003, *Earth Planetary Sci. Lett.* **205**(3−4), 123−138.

Bourrouilh, R.: 2001, in M. Gargaud, D. Despois and J.-P. Parisot (eds.), *Evolution parallèles de la Terr et de la Vie. L*'environnement de la Terre primitive, Presses Universitaires de Bordeaux, Bordeaux, pp. 287−320.

Brasier, M. D., Green, O. R., Jephcoat, A. P., Kleppe, A. K., Van Kranendonk, M. J., Lindsay, J. F., Steele, A. and Grassineau, N. V.: 2002, *Nature* **416**, 76−81.

Brocks, J. J., Buick, R., Logan, G. A. and Summons, R. E.: 2003a, *Geochemica et Cosmochemica Acta* **67**, 4289−4319.

Brocks, J. J., Logan, G. A., Buick, R. and Summons, R. E.: 1999, *Science* **285**, 1033−1036.

Brocks, J. J., Buick, R., Summons, R. E. and Logan, G. A.: 2003, *Geochimica et Cosmochimica Acta* **67**(22), 4321−4335.

Brown, G. C.: 1985, in N. Snelling (ed.), *The Chronology of the Geological Record*, Memoir - Geological Society of London, London, pp. 326−334.

Buick, R.: 1992, *Nature* **255**, 74−77.

Byerly, G. R. and Lowe, D. R.: 1994, *Geochemica et Cosmochemica Acta* **58**(16), 3469−3486.

Canfield, D. E. and Teske, A.: 1996, *Nature* **382**, 127−132.

Catling, D. C. and Claire, M. W.: 2005, *Earth Planetary Sci. Lett.* **237**, 1−20.

Catling, D. C., Zahnle, K. J. and McKay, C. P.: 2001, *Science* **293**, 839−843.

Chadwick, B., Claeys, P. and Simonson, B.: 2001, *J. Geol. Soc. London* **158**, 331−340.

Channer, D. M. D. R., de Ronde, C. E. J. and Spooner, E. T. C.: 1997, *Earth Planetary Sci. Lett.* **150**, 325−335.

Commeyras, A., Taillades, J., Collet, H., Boiteau, L., Vandenabeele-Trambouze, O., Pascal, R., Rousset, A., Garrel, L., Rossi, J., Biron, J., Lagrille, O., Plasson, R., Souaid, E., Danger, G., Selsis, F., Dobrijévic, M. and Martin, H.: 2004, *Origins Life Evol. Biosphere* **34**, 35−55.

Condie, K. C.: 1989. *Plate Tectonics and Crustal Evolution*, Pergamon, Oxford, 476 pp.

Condie, K. C.: 1998, *Earth Planetary Sci. Lett.* **163**(1−4), 97−108.

Cornell, D. H., Schütte, S. S. and Elington, B. L.: 1996, *Precambrian Res.* **79**, 101−123.

Cowen, R.: 2005, The History of Life, 4th edn. Blackwell Scientific, 324 pp.

Culler, T. S., Becker, T. A., Muller, R. A. and Renne, P. R.: 2000, *Science* **287**, 1785−1788.

de Ronde, C. E. J., Channer, D. M. d., Faure, K., Bray, C. J. and Spooner, T. C.: 1997, *Geochimica and Cosmochimica Acta* **61**(19), 4025−4042.

Delano, J. W.: 2001, *Origins Life Evol. Biosphere* **31**(4−5), 311−341.

Des Marais, D. J.: 2000, *Science* **289**, 1703−1705.

Des Marais, D. J., Strauss, H., Summons, R. E. and Hayes, J. M.: 1992, *Nature* **359**, 605−609.

Dypvik, H., Burchell, M. J. and Claeys, P.: 2003, in H. Dypvik, M. J. Burchell and P. Claeys (eds.), *Cratering in Marine Environments and on Ice*, Springer, Berlin, pp. 1−19.

Beukes, N. J. and Kirschvink, J. L.: 1997, *Nature* **386**, 262−266.

Farquhar, J., Bao, H. M. and Thiemens, M.: 2000, *Science* **289**(5480), 756−758.

Farquhar, J., Savarino, J., Airieau, S. and Thiemens, M. H.: 2001, *J. Geophys. Res. Planets* **106**(E12), 32829−32839.

Farquhar, J. and Wing, B. A.: 2003, *Earth Planetary Sci. Lett.* **213**, 1−13.

Farquhar, J., Wing, B. A., McKeegan, K. D., Harris, J. W., Cartigny, P. and Thiemens, M. H.: 2002, *Science* **298**, 2369−2372.

Foriel, J., Philippot, P., Rey, P., Somogyi, A., Banks, D. and Menez, B.: 2004, *Earth Planetary Sci. Lett.* **228**, 451−463.

Frape, S. K., Blyth, A., Blomqvist, R. and McNutt, R. H.: 2003, in J. I. Drever (ed.), *Deep fluids in the continents: II Crystalline rocks. The Oceans and Marine Geochemistry. Treatise of Geochemistry*, Elsevier-Pergamon, Oxford, pp. 541−580.

Fritz, P. and Frape, S.K. (eds.), 1987. *Saline Water and Gases in Crystalline Rocks. GAC Special Paper, 33*, Geological Association of Canada, Ottawa, 259 pp.

Gladman, B., Dones, L., Levison, H. F. and Burns, J. A.: 2005, *Astrobiology* **5**(4), 483−496.

Glass, B. P. and Burns, C. A.: 1988, *Proc. Lunar Planetary Sci. Conf.*, 455−458.

Glikson, A. Y.: 1999, *Geology* **27**(5), 387−390.

Glikson, A. Y.: 2001, *J. Geodynamics* **32**(1−2), 205−229.

Gomes, R., Levison, H. F., Tsiganis, K. and Morbidelli, A.: 2005, *Nature* **435**, 466−469.

Gordon, R. M., Martin, J. H. and Knauer, G. A.: 1982, *Nature* **299**, 611−612.

Gorman, B. E., Pearce, T. H. and Birkett, T. C.: 1978, *Precambrian Res.* **6**, 23−41.

Gough, D. O.: 1981, *Solar Phys.* **74**, 21−34.

Graedel, T. E. and Keene, W. C.: 1996, *Pure Appl. Chem.* **68**, 1689−1697.

Gutscher, M.-A., Maury, F., Eissen, J.-P. and Bourdon, E.: 2000, *Geology* **28**(6), 535−538.

Gutzmer, J., Banks, D., Lüders, V., Hoefs, J., Beukes, N. J. and von Bezing, K. L.: 2003, *Chem. Geol.* **201**, 37−53.

Gutzmer, J., Pack, A., Luders, V., Wilkinson, J.-J., Beukes, N. J. and van Niekerk, H. S.: 2001, *Contrib. Mineral. Petrol.* **142**, 27−42.

Hanna, J. L., Bekker, A., Stein, H. J. J., Markey, R. J. and Holland, H. D.: 2004, *Earth Planetary Sci. Lett.* **225**, 43−52.

Hassler, S. W., Robey, H. F. and Simonson, B.: 2000, *Sedimentary Geol.* **135**, 283−294.

Hassler, S. W. and Simonson, B. M.: 2001, *J. Geol.* 109.

Hilburn, I. A. L. J., Kirschvink, J. L. E. T., Tada, R., Hamano, Y. and Yamamoto, S.: 2005, *Earth Planetary Sci. Lett.* **232**(3−4), 315−332.

Hoffman, P. F., Kaufman, A. J., Halverson, G. P. and Schrag, D. P.: 1998, *Science* **281**, 1342−1346.

Holland, H. D.: 1984. *The Chemical Evolution of the Atmosphere and Oceans*, Princeton Series in Geochemistry. Princeton University Press, Princeton, 582 pp.

Holland, H. D. 1994, in S. Bengston (ed.), *Early Life on Earth*. Columbia University Press, New York, pp. 237−244.

Holland, H. D.: 1999, *The Geochemical News* **100**, 20−22.

Holland, H. D.: 2002, *Geochimica et Cosmochimica Acta* **66**(21), 3811−3826.

Holland, H. D.: 2003, in H. D. Holland and K. K. Turekian (eds.), *The Oceans and Marine Geochemistry. Treatise of Geochemistry*, Elsevier-Pergamon, Oxford, pp. 583−625.

Horibe, Y., Endo, K. and Tsubota, H.: 1974, *Earth Planetary Sci. Lett.* **23**(1), 136−140.

Isley, A. E.: 1995, *J. Geol.* **103**, 169−185.

Johnson, N. M. and Fegley, B. Jr.: 2002, *Adv. Space Res.* **29**, 2333−241.

Kamber, B. S. and Webb, G. E.: 2001, *Geochimica et Cosmochimica Acta* **65**, 2509−2525.

Karhu, J. A. and Holland, H. D.: 1996, *Geology* **24**, 867−870.

Kasting, J. F.: 1993, *Earth*'s Early Atmosphere **259**, 920−926.

Kasting, J. F.: 2005, *Precambrian Res.* **137**, 119−129.

Kasting, J. F., Eggler, D. H. and Raeburn, S. P.: 1993, *J. Geol.* **101**, 245−257.

Knauth, L. P.: 1998, *Nature* **395**, 554−555.

Knauth, L. P.: 2005, *Palaeogeogr. Palaeoclimatol. Palaeoecol.* **219**(1−2), 53−69.

Knauth, L. P. and Lowe, D. R.: 1978, *J. Geol.* **41**, 209−222.

Knauth, L. P. and Lowe, D. R.: 2003, *Geol. Soc. Am. Bull.* **115**(5), 566−580.

Knoll, A. H.: 2003, *Deobiology* **1**, 3−14.

Konkauser, K. O., Hamade, T., Morris, R. C., Ferris, G. F., Southam, G. and Canfield, D. E.: 2002, *Geology* **30**, 1079−1082.

Kopp, R. E., Kirschvink, J. L., Hilburn, I. A. and Nash, C. Z.: 2005, *Proc. Nat. Acad. Sci.* **102**, 11131−11136.

Krauskopf, K. B. and Bird, D. K.: 1995. *Introduction to Geochemistry*, McGraw-Hill, New York, 647 pp.

Kress, M. E. and McKay, C. P.: 2004, *Icarus* **168**(2), 475−483.

Kyte, F. T., Shukolyukov, A., Lugmair, G. W., Lowe, D. R. and Byerly, G. R.: 2003, *Geology* **31**, 283−286.

Kyte, F. T. and Bostwick, J. A.: 1995, *Earth Planetary Sci. Lett.* **132**(1−4), 113−127.

Li, Z.-X. A. and Lee, C.-T. A.: 2004, *Earth Planetary Sci. Lett.* **228**, 483−493.

Libourel, G., Marty, B. and Humbert, F.: 2003, *Geochimica et Cosmochimica Acta* **67**, 4123−4135.

Lowe, D. R. and Byerly, G. R.: 2003, *Geology* **31**(10), 909−912.

Lowe, D. R., Byerly, G. R., Kyte, F. T., Shukolyukov, A., Asaro, F. and Krull, A.: 2003, *Astrobiology* **3**(1), 7−48.

Maher, K. A. and Stevenson, D. J.: 1988, *Nature* **331**, 612−614.

Martin, H.: 1986, *Geology* **14**, 753−756.

Martin, H.: 1999, *Lithos* **46**(3), 411−429.

Martin, H. and Moyen, J.-F.: 2002, *Geology* **30**(4), 319−322.

Martin, H., Smithies, R. H., Rapp, R., Moyen, J.-F. and Champion, D.: 2005, *Lithos* **79**(1−2), 1−24.

Marty, B. and Dauphas, N.: 2003, *Earth Planetary Sci. Lett.* **206**, 397−410.

McCulloch, M. T. and Bennet, V. C.: 1993, *Lithos* **30**, 237−255.

McCulloch, M. T. and Bennett, V. C.: 1994, *Geochimica and Cosmochimica Acta* **58**, 4717−4738.

Melezhik, V. A., Fallick, A. E., Hanski, E. J., Kump, L. R., Lepland, A., Prav, A. R. and Strauss, H.: 2005, *Geol. Soc. Am. Today* **15**(11), 4−11.

Mojzsis, S. J., Coath, C. D., Greenwood, J. P., McKeegan, K. D. and Harrison, T. M.: 2003, *Geochimica et Cosmochimica Acta* **67**, 1635−1658.

Montanari, A. and Koeberl, C.: 2000. *Impact Stratigraphy Lecture Notes in Earth Sciences, 93*, Springer Verlag, Berlin, 364 pp.

Moyen, J.-F., Jayananda, M., Nédelec, A., Martin, H., Mahabaleswar, B. and Auvray, B.: 2003, *J. Geol. Soc. India* **62**, 753−758.

Moyen, J.-F., Martin, H. and Jayananda, M.: 1997, *Compte Rendus de l'*Académie des Sciences de Paris **325**, 659−664.

Navarro-Gonzalez, R., McKay, C. P. and Nna Mvondo, D.: 2001, *Nature* **412**, 61−64.

Nhleko, N.: 2004, *The Pongola Supergroup in Swaziland*. Rand Afrikaans University.

Nijman, W., de Bruijne, K. C. H. and Valkering, M. E.: 1998, *Precambrian Res.* **88**(1−4), 25−52.

Nisbet, E. G., Cheadle, M. J., Arndt, N. T. and Bickle, M. J.: 1993, *Lithos* **30**, 291−307.

Nisbet, E. G. and Fowler, C. M. R.: 2003, in W. H. Schlesinger (ed.), *Biogeochemistry. Treatise of Geochemistry*, Elsevier-Pergamon, Oxford, pp. 1−61.

Nisbet, E. G. and Sleep, N. H.: 2001, *Nature* **409**, 1083−1091.

Oberbeck, V. and Fogelman, G.: 1989, *Nature* **339**, 434.

Pavlov, A. A., Hurtgen, M. T., Kasting, J. F. and Arthur, M. A.: 2003, Geology **31**, 87−90.

Pavlov, A. A. and Kasting, J. F.: 2002, *Astrobiology* **2**(1), 27−41.

Pavlov, A. A., Kasting, J. F., Brown, L. L., Rages, K. A. and Freedman, R.: 2000, *J. Geophys. Res.* **105**, 11981−11990.

Peltier, W. R., Butler, S. and Solheim, L. P.: 1997, in D. J. Grossley (ed.), *Earth's Deep Interior*, Gordon and Breach, Amsterdam, pp. 405−430.

Pinti, D. L.: 2005, in M. Gargaud, B. Barbier, H. Martin and J. Reisse (eds.), *Lectures in Astrobiology. Advances in Astrobiology and Biogeophysics*, Springer-Verlag, Berlin, pp. 83−107.

Pinti, D. L., Hashizume, K. and Matsuda, J.: 2001, *Geochimica et Cosmochimica Acta* **65**(14), 2301−2315.

Pinti, D. L., Hashizume, K., Philippot, P., Foriel, J. and Rey, P.: 2003, Geochimica et Cosmochimica Acta, A287.

Rapp, R. P., Shimizu, N. and Norman, M. D.: 2003, *Nature* **425**, 605−609.

Rapp, R. P., Shimizu, N., Norman, M. D. and Applegate, G. S.: 1999, *Chem. Geol.* **160**, 335−356.

Rasmussen, B. and Koeberl, C.: 2004, *Geology* **32**, 1029−1032.

Ribas, I., Guinan, E. F., Gudel, M. and Audard, M.: 2005, *The Astrophis J.* **622**(1), 680−694.

Robin, E., Bonté, P., Froget, L., Jéhanno, C. and Rocchia, R.: 1992, *Earth Planetary Sci. Lett.* **108**, 181−190.

Roedder, E.: 1984. *Fluid Inclusions*, Rewiews in Mineralogy 12., Mineralogical Society of America.

Rosing, M. T.: 1999, *Science* **283**, 674−676.

Rosing, M. T. and Frei, R.: 2004, *Earth Planetary Sci. Lett.* **217**, 237−244.

Rouxel, O. J., Bekker, A. and Edwards, K. J.: 2005, *Science* **307**, 1088−1091.

Rye, R. and Holland, H. D.: 1998, *Am. J. Sci.* **298**, 621−672.

Sagan, C. and Mullen, G.: 1972, *Science* **177**, 52−56.

Samaniego, P., Martin, H., Robin, C. and Monzier, M.: 2002, *Geology* **30**(11), 967−970.

Samaniego, P., Martin, H., Robin, C., Monzier, M. and Cotten, J.: 2005, *J. Petrol.* **46**, 2225−2252.

Selsis, F.: 2000, Evolution of the atmosphere of terrestrial planets. From early Earth atmo-sphere to extrasolar planets. Ph. D. Thesis, University of Bordeaux.

Selsis, F.: 2002, Occurrence and detectability of O_2-rich atmosphere in circumstellar "habit-able zones". ASP 269: The Evolving Sun and its Influence on Planetary Environments.

Selsis, F.: 2004. *The Prebiotic Atmosphere of the Earth., Astrobiology, Future Perspective*, Kluwer, Astrophysics and Space Science Library.

Schrag, D. P., Berner, R. A., Hoffman, P. F. and Halverson, G. P.: 2002. *Geochem. Geophys. Geosyst.*, **3**(6), doi: 10.1029/2001GC000219.

Shen, Y. and Buick, R.: 2004, *Earth-Sci. Rev.* **64**(3–4), 243–272.

Shen, Y., Pinti, D. L. and Hahsizume, K.: 2006, in K. Benn, J.-C. Mareschal and K. Condie (eds.), *Archean Geodynamics and Environments. AGU Geophysical Monograph*, American Geophysical Union, Washington, DC, Vol 164, pp. 305–320.

Shirey, S. B. and Hanson, G. N.: 1984, *Nature* **310**, 222–224.

Shukolyukov, A., Castillo, P. and Simonson, B. W. L. G., 2002. Chromium in Late Archean spherule layers from Hamersley basin, Western Australia; isotopic evidence for extrater-restrial component, Lunar and Planetary Science Conference, Houston, Texas, pp. 1369 (abstract).

Shukolyukov, A., Kyte, F. T., Lugmair, G. W., Lowe, D. R. and Byerly, G. R.: 2000, in I. Gilmour and C. Koeberl (eds.), *Impacts and the Early Earth*, Springer, Berlin, pp. 99–115.

Simonson, B.: 2003, *Astrobiology* **3**(1), 49–65.

Simonson, B., Hassler, S. W., Smit, J. and Summer, D.: 2004, How Many Late Archean Impacts are Recorded in the Hamersley Basin of Western Australia, Lunar and Planetary Science, Houston Texas, pp. CD-ROM 1718 [Abstract].

Simonson, B. M.: 1992, *Geol. Soc. Am. Bull.* **104**, 829–839.

Simonson, B. M. and Glass, B. P.: 2004, *Ann. Rev. Earth Planet Sci.* **32**, 329–361.

Simonson, B. M. and Harnik, P.: 2000, *Geology* **28**(11), 975–978.

Simonson, B. M., Hassler, S. W. and Beukes, N. J.: 1999, Late Archean impact spherule layer in South Africa that may correlate with a Western Australian layer. Geological Society of America, Special paper 339.

Sleep, B. E. and McClure, P. D.: 2001, *J. Contam. Hydrol.* **50**(1–2), 21–40.

Sleep, N. H., Meibom, A., Fridriksson, T., Coleman, R. G. and Bird, D. K.: 2004, *Proc. Nat. Acad. Sci.* **101**(35), 12818–12823.

Sleep, N. H. and Zahnle, K.: 2001a, *J. Geophys. Res. Planets* **106**(E1), 1373–1399.

Sleep, N. H., Zahnle, K. and Neuhoff, P. S.: 2001, *Proc. Nat. Acad. Sci. USA* **98**(7), 3666–3672.

Sleep, N. H. and Zahnle, K. J.: 2001b, *J. Geophys. Res.* **106**, 1373–1400.

Smit, J.: 1999, *Ann. Rev. Earth Planetary Sci.* **27**, 75–113.

Smit, J., Alvarez, W., Montanari, A., Swinburne, N., Van Kempen, T. M., Klaver, G. T. and Lustenhouwer, W. J.: 1992, *Proc. Lunar Planetary Sci.* **22**, 87–100.

Smithies, R. H.: 2000, *Earth Planetary Sci. Lett.* **182**, 115–125.

Stein, M. and Hofmann, A. W.: 1994, *Nature* **372**, 63–68.

Svetov, S. A., Svetova, A. I. and Huhma, H.: 2001, *Geochem. Int.* **39**, 24–38.

Tian, F., Toon, O. B., Pavlov, A. A. and De Sterck, H.: 2005, *Science* **308**, 1014–1017.

Ueno, Y., Yoshioka, H., Maruyama, S. and Isozaki, Y.: 2004, *Geochimica et Cosmochimica Acta* **68**(3), 573–589.

Van Kranendonk, M. J., Hickman, A. H., Williams, I. R. and Nijman, W.: 2001, Archaean geology of the East Pilbara granite-greenstone terrane, Western Australia − A field guide, Geological Survey of Western Australia, Perth.

Veizer, J. and Compston, W.: 1976, *Geochimica et Cosmochimica Acta* **40**, 905–914.

Veizer, J., Hoefs, J., Ridler, R. H., Jensen, L. S. and Lowe, D. R.: 1989, *Geochimica et Cosmochimica Acta* **53**, 845−857.

von Damm, K. L., Oosting, S. E., Kozlowski, R., Buttermore, L. G., Colodner, D. C., Edmonds, H. N., Edmond, J. M. and Grebmeir, J. M.: 1995, *Nature* **375**, 47−50.

Walker, J. C. G., Hays, P. B. and Kasting, J. F.: 1981, *J. Geophys. Res.* **86**, 9776−9782.

Wallace, M. W., Gostin, V. A. and Keays, R. R.: 1990, *Geology* **18**(2), 132−135.

Weiershauser, L. and Spooner, E. T. C.: 2005, *Precambrian Res.* **138**(1−2), 89−123.

Weiss, R. F.: 1970, *Deep-Sea Res.* **17**, 721−735.

Wells, L. E., Armstrong, J. C. and Gonzalez, G.: 2003, *Icarus* **162**, 38−46.

Young, G. M., von Brunn, V., Gold, D. J. C. and Minter, W. E. L.: 1998, *J. Geol.* **106**, 523−538.

Zahnle, K. and Sleep, N. H.: 2002, in C. M. R. Fowler, C. J. Ebinger and C. J. Hawkesworth (eds.), *The Early Earth: Physical, Chemical and Biological Development*, Geological Society, London, pp. 231−257.

Zegers, T. E., de Wit, M. J., Dann, J. and White, S. H.: 1998, *Terra Nova* **10**, 250−259.